
Université d'Ottawa · University of Ottawa

# Université d'Ottawa · University of Ottawa

FACULTÉ DES ÉTUDES SUPÉRIEURES ET POSTDOCTORALES

FACULTY OF GRADUATE AND POSTDOCTORAL STUDIES

CRISAN, Simona

AUTEUR DE LA THÈSE - AUTHOR OF THESIS

M.Sc. (Physics)

GRADE - DEGREE

Department of Physics

FACULTÉ, ÉCOLE, DÉPARTEMENT - FACULTY, SCHOOL, DEPARTMENT

TITRE DE LA THÈSE - TITLE OF THE THESIS

A Theoretical Investigation of the Relaxation of Random Linear Polymers and of the Elasticity of Single Polymer Chains

G. Slater

DIRECTEUR DE LA THÈSE - THESIS SUPERVISOR

EXAMINATEURS DE LA THÈSE - THESIS EXAMINERS

B. Carnegie

L. Chen

I. L'Heureux

J.-M. De Koninck, Ph.D.

LE DOYEN DE LA FACULTÉ DES ÉTUDES SUPÉRIEURES ET POSTDOCTORALES

SIGNATURE

DEAN OF THE FACULTY OF GRADUATE AND POSTDOCTORAL STUDIES

# A theoretical investigation of the relaxation of random linear polymers and of the elasticity of single polymer chains

by

**Simona Silvia Crisan**

Thesis submitted to
University of Ottawa for the degree of
**Master of Science in Physics**

Department of Physics
Faculty of Science
University of Ottawa

*Your file Votre référence*
*ISBN: 0-612-90053-3*
*Our file Notre référence*
*ISBN: 0-612-90053-3*

# Summary

Polymeric and biological disordered materials are characterized by unique dynamical features. Although the details of the physical dynamical mechanisms are different, the disorder seems to be a common cause for non-exponential relaxation in these materials. The numerous experimental results which reveal a rather universal form of relaxation, namely a KWW or stretched exponential type function ( $e^{-(t/\tau)^{\beta}}$ , $\beta<1$) have not yet been adequately explained by a unified theory. Such a disordered polymeric system is studied in this thesis and its relaxation is analysed in the framework of the well known Rouse model. This model allows for exact solutions and different types of disorder are analysed here. Exact solution and a good control over the disorder provide us with a fundamental description of the transition towards KWW behaviour. Our results favor a theory of relaxation based on parallel relaxation modes.

The second part of the thesis focuses on the elasticity of a single polymer chain. The correct statistical mechanical ensemble associated with an experimental measurement probing single chain properties is an issue of great interest given the breakthroughs in the development of methods which can directly probe single chain mechanics. The complicated force-extension expressions obtained for a chain subjected to spatial constraints are available only as approximations, even for ideal models. The use of such relations in theoretical studies as well as in computer simulations is cumbersome and time consuming. A systematic method to construct simpler but still accurate expressions for the force function is given. As we demonstrate, these approximations can provide expressions with an arbitrary degree of accuracy and the proper mean statistical properties.

# Sommaire

Les matériaux souples polymériques et biologiques se distinguent par leur comportement dynamique unique. Malgré la diversité des mécanismes qui entrent en jeux, le désordre inhérent à ces systèmes donne lieu à des phénomènes de relaxation non-exponentiels. Les nombreux résultats expérimentaux à ce sujet peuvent être représentés de façon presque universelle par des fonctions exponentielles étirées ou de type KWW, mais aucune théorie n'arrive à les expliquer de façon unifiée. Cette thèse étudie les phénomènes de relaxation engendrés par différents types de désordre dans un système polymérique, à l'aide du modèle de Rouse. Le contrôle du désordre et les solutions analytiques exactes obtenues dans le cadre de ce modèle apportent une compréhension fondamentale de la transition vers le régime KWW. Les résultats obtenus favorisent une théorie basée sur la notion de modes de relaxation parallèles.

La deuxième partie de la thèse porte sur l'élasticité d'une chaîne polymérique isolée. La description de ce sytème en terme d'un ensemble statistique approprié est d'un grand intérêt en regard de l'avènement de nouvelles méthodes expérimentales permettant justement de mesurer directement les propriétés mécaniques individuelles d'une macromolécule. Les expressions compliquées généralement utilisées pour relier la force appliquée à l'étirement de la chaîne (expressions qui d'ailleurs demeurent approximatives, même dans le cas de modèles idéaux) ne se prêtent pas aisément à un traitement théorique et s'avèrent inefficaces pour des calculs numériques. Une nouvelle méthode systématique pour générer des fonctions de réponse plus simples mais tout aussi justes est présentée ici. Ces nouvelles approximations permettent d'atteindre un niveau de précision arbitrairement élevé et reproduisent fidèlement, d'un point de vue statistique, les propriétés d'une chaîne polymérique.

# Acknowledgments

I would like to express my appreciations to Dr. Gary Slater, who supervised my work with professionalism and carefulness. I am grateful to him for introducing me to the field of polymers. During my work with him I really enjoyed his cheerfulness and optimism.

I also want to thank to my office colleagues for the good work atmosphere they created and for their help in various situations. I am especially thankful to Frederique Tessier for his kindness.

The discussions with my friend Catalin Rada on various mathematical subjects were very useful for my work. Also I am grateful to my colleague and friend Roxana Flacau for her optimistic support in any situation.

Finally I thank my husband for his support, constructive criticism and suggestions.

# Table of contents

# Chapter 1

This thesis is structured in two parts. The first one studies the influence of the compositional disorder on the dynamics of linear polymer chains. The second part is related to the mechanical elastic properties of a single linear chain.

## 1.1 The thesis topics and the field of polymer physics

A polymer can exist in a condensed state, either crystalline or amorphous, or in a dispersed state, a solution. In the former one, the polymer may be found in one of three different states that depend on the external conditions and on the production. At low temperature there are crystalline and amorphous polymers (the last one is usually called glassy polymers). At higher temperatures the polymers are into viscoelastic, rubber-like state. Finally above the flow temperature, polymers acquire the properties of a viscous liquid. In solution each polymer molecule is surrounded by solvent molecules. The properties of this state depend mostly on the concentration of the solution. In a dilute state the polymers do not mutually overlap. The subjects of this thesis correspond to the dilute solution limit.

A polymer in a solution changes its shape continuously. The number of conformations it can take depends on its flexibility. The most flexible model, the freely jointed chain, is used in this thesis.

The length scale of the molecular motions in polymers can range increasingly from the very short, through the intermediate and long, up to the longest terminal relaxation that involves the entire chain. The first involves a compact part of the monomer, like that of a $CH_3$ methyl group or slightly larger. The intermediate one comprises more than one monomer and is usually called "segmental motion". The longest scale deals with different parts of the chain. In the present work, we focus our attention on the long length scale domain, simply described by the bead-spring model (widely known as the Rouse model). The time scale generally extends from the local

modes (involved in the glass transition) to chain flow, the latter being free for dilute solutions and hindered by entanglements for concentrated solutions.

For the dynamics of a polymer chain in solution, the equilibrium case is considered in this work. In order to describe the behaviour of the polymer, correlation and relaxation functions are used as they correspond to experimentally measurable quantities. The relaxation function measures the response of the system to an applied perturbation. If the perturbation is small the response is linear. On the other hand, the correlation function is related to fluctuating quantities and it measures the time correlation of a physical observable in a statistical way. If, under a small perturbation a system does not move appreciable from the equilibrium state, the fluctuation-dissipation theorem directly relates the two functions. The relaxation function gives the time evolution of the correlation function. In equilibrium, the fluctuations decay with the same time dependence irrespective to the presence or absence of small perturbations. The above conditions are assumed to apply to the present work, when we study the conformational relaxation.

The most popular relaxation function is the Debye function

$$\Phi(t) = \Phi_0 \exp(-t/\tau) \tag{1.1}$$

and it can be explained in terms of barrier models: the equilibrium is achieved by overcoming well-defined and uniform potential barriers. This situation usually applies for crystalline materials, but is not necessarily valid in complex systems. A non-exponential relaxation is more appropriate in this case, although we do not yet have a good microscopic understanding of these phenomena. The most common function is a sub-unitary exponential, usually called stretched exponential,

$$\Phi(t) = \Phi_0 \exp\left[-\left(\frac{t}{\tau}\right)^{\beta}\right] \tag{1.2}$$

where $\beta$ takes values between 0 and 1. This form is widely adopted as an empirical fitting function. This function was used to describe stochastic processes (Ref. 21) but also cooperatively relaxing systems (Ref. 5), or self-retarding processes in which the KWW (Kohlrausch-William-Watts) characteristic time $\tau$ changes with time (Ref. 29). The ubiquitous character of this function is not yet justified by a complete microscopic theory. Currently, there is an incomplete agreement in the literature as to the appropriate interpretation of non-exponential relaxation phenomena in polymers. Both strongly interacting systems and systems with disorder exhibit non-exponential

relaxation in the form of Eq. 1.2. For example, the randomness of the structure in some type of randomly branched polymers is invoked as a plausible cause of their stretched exponential decay (Refs. 7,8,9). The results presented in Chapter 4 examine how intramolecular disorder can lead to non-exponential relaxation in linear polymers, in the absence of the interchain interactions.

Although there is a huge amount of experimental and simulation data about non-exponential relaxation, there are few theoretical alternatives in the literature. A discussion of some of these theories can be found in Chapter 3.

For real polymers, the hydrodynamic interaction has to be considered, (i.e. the coupling of the motion of the different parts of the polymers via the surrounding fluid). More sophisticated models (e.g., the Zimm model) include these effects in the total potential energy of the polymer. However, although important improvements regarding some scaling laws are then achieved, the form of the relaxation function is not affected, at least in the long time limit. Some authors have indeed included hydrodynamics in their dynamical simulations, but their results show negligible differences from the Rouse model (Ref. 28). In our study, we neglect both the hydrodynamic and the excluded volume interactions for the sake of simplicity, and because we want to use an exactly solvable model.

## 1.2 Polymer stretching

The elastic behaviour of single polymer chains plays an important role in the mechanical proprieties of polymeric materials. A good understanding of the macro-elasticity of a network, for example, requires a microscopic study of single chain elasticity. Recent technical developments permit the manipulation of single polymer chains and force-extension measurements can directly test models of polymer elasticity. It is sometimes stated that ensembles corresponding to a fixed end-to-end vector or to fixed stretching forces acting at the chain ends can lead to distinct elasticity laws. Atomic force microscopy can be used to measure the average contractile force for an imposed end-to-end chain extension. Similarly, the average position of one chain end can be determined, if external forces are applied to it, when the other end is fixed (for example, chemically adsorbed to a support).

The theoretical treatment of the force–extension relation rises mathematical difficulties even for simple models that takes into account the finite extensibility of the chain. The evaluation is especially difficult in the ensemble with the fixed end-to-end distance. The need for such force-extension laws in analytical studies as well as in computer simulations requires the use of simplified and approximate expressions. In the last chapter of the thesis, a method to generate analytical approximations for the case of the fixed end-to-end distance ensemble is presented. These approximate relations preserve the form of the exact expression in both the small and large extension limits and minimize the errors in the intermediate extensions. However, the anharmonic character of these forces, when included into the chain potential energy, changes the equilibrium statistics of the chain. A quantitative evaluation of this effect is given in our work.

## 1.3 Outline of the thesis

The thesis is structured as follows. In chapter 2 we summarise some statistical proprieties of polymer chains and present the Rouse model. The current theoretical status of the non-exponential decay problem is presented in chapter 3. Three relevant theories, specific to certain systems, are outlined, together with an attempt for a unifying explanation. A model for a disordered linear polymer is introduced in chapter 4 and a numerical study of its relaxation is carried out. In the last chapter, the problem of single chain elasticity is treated. Analytical rational approximations are developed as simpler alternatives to existing force-extension relations in the strain ensemble.

# Chapter 2

# Fundamentals

## 2.1 Statistical properties of polymers

In this section we briefly overview some basic concepts regarding the statistics of polymer chains, concepts that are required for an adequate understanding of this thesis.

From the statistical point of view a polymer or a macromolecule is a collection of atoms, connected in a specific way by covalent bonds. When, subject to certain environmental conditions, a macromolecule is free to change its shape, we are in the field of flexible polymers. Studying the dynamics of these molecules requires a detailed description of the conformation, i.e. the position of each atom of the chain. However, the location of each atom in the macromolecule is both cumbersome and excessive for the overwhelming majority of purposes. Therefore, various quantities are used to describe the conformation of a polymer in a statistical way. These are typically the scalar magnitude of the vector $\vec{h}$ connecting the ends of the chain (more easily defined for linear polymers) and the radius of gyration $R_g$, defined as the root-mean-square distance of the collection of atoms from their common centre of gravity. The coresponding mathematical expressions depend on the specific model used for the polymer. Several such models exist and they are developed gradually starting from the most idealised and simplified one to the closest approach to known real conditions. "Bond" and "joints" or "beads" in these models can represent real atoms and real chemical bonds or they may include many of them in a single unit.

When a linear polymer is viewed as sequence of equivalent rigid links of length b, each freely pointing in space independently of the previous link direction, we talk about the freely jointed chain model (FJC). If the vectors $\vec{R}_0, \vec{R}_1, ..., \vec{R}_N$ give the position of the N+1 joints, the mean square value of $\vec{h}$ is written as

$$\left\langle h^2 \right\rangle = \left\langle \vec{h} \cdot \vec{h} \right\rangle = \left\langle \sum_{i,j}^{N} \vec{b}_i \cdot \vec{b}_j \right\rangle = \sum_{i}^{N} \left\langle b_i^2 \right\rangle + 2 \sum_{0<i<j\le N} \left\langle \vec{b}_i \cdot \vec{b}_j \right\rangle \tag{2.1}$$

where $\vec{b}_i = \vec{R}_i - \vec{R}_{i-1}$. Then the absence of the correlation between links, e.g.

$$\left\langle \vec{b}_i \cdot \vec{b}_j \right\rangle = 0, \quad i \neq j \quad , \tag{2.2}$$

leads to the famous result

$$\left\langle h^2 \right\rangle = Nb^2 . \tag{2.3}$$

A chain with fixed bond angles $\theta$, in addition to fixed bond lengths, forms a freely rotating chain. Each bond can freely rotate about the adjacent one. The correlation between the bonds gives

$$\left\langle \vec{b}_i \cdot \vec{b}_{i+k} \right\rangle = b^2 (\cos\theta)^k \tag{2.4}$$

which in the long chain limit (N>>1) gives

$$\left\langle h^2 \right\rangle = Nb^2 \frac{1+\cos\theta}{1-\cos\theta} . \tag{2.5}$$

The scaling relation

$$\left\langle h^2 \right\rangle \propto N \tag{2.6}$$

thus holds for both models. The length $b_k$ for which Eq.2.3 is still fulfilled is called the effective bond length. In fact, $b_k$ is the ratio between the mean square end-to-end distance and the maximum length $h_{max}$=Nb,

$$b_K = \frac{\left\langle h^2 \right\rangle}{h_{\max}} = b \frac{1+\cos\theta}{1-\cos\theta} \tag{2.7}$$

and it describes the stiffness of the polymer. It is also known as the Kuhn statistical segment length.

The distribution function of the end-to-end distance $\vec{h}$ is Gaussian in the limit of long chains, i.e.

$$\Phi(\vec{h}, N) = (3/2\pi Nb^2)^{3/2} \exp(-\frac{3h^2}{2Nb^2}) \tag{2.8}$$

Again this expression holds for several models if the proper effective segment length is used.

Besides the FJC, these properties are obviously satisfied for a chain made of segments whose lengths satisfy a Gaussian distribution

$$\psi(\vec{b}) = (3/2\pi b^2)^{3/2} \exp(-\frac{3b^2}{2b_0^2}), \tag{2.9}$$

where $b_0$ is the mean length of the segments. We note that $\vec{b}$ is a variable here.

The Gaussian chain has an important property: the distribution of the vector $\vec{R}_n - \vec{R}_m$ between any two units of the chain is Gaussian,

$$\Phi(\vec{R}_n - \vec{R}_m) = (3/2\pi b^2|n-m|)^{3/2} \exp\left[-\frac{3(\vec{R}_n - \vec{R}_m)^2}{2|n-m|b_0^2}\right]. \tag{2.10}$$

This result is fully consistent with the well known scaling expression

$$\left\langle (\vec{R}_n - \vec{R}_m)^2 \right\rangle = |n-m|b_0^2 . \tag{2.11}$$

An equivalent physical picture of the Gaussian chain is a collection of beads connected by harmonic springs. The potential energy of such a chain is the harmonic form

$$U(\{\vec{R}_n\}) = \frac{3k_BT}{2b_0^2}\sum_{n=1}^{N}(\vec{R}_n - \vec{R}_m)^2 . \tag{2.12}$$

This can be easily derived from the Boltzmann probability factor for a specific chain conformation

$$\left(\frac{3}{2\pi b_0^2}\right)^{3N/2} \exp\left(-\sum_{n=1}^{N}\frac{3(\vec{R}_n - \vec{R}_m)^2}{2b_0^2}\right). \tag{2.13}$$

Unfortunately, we also see that the Gaussian distribution function gives small but finite probabilities for the non-realistic situation of the conformations with $h>h_{max}= Nb_0$.

## 2.2 The Rouse model

### 2.2.1 The equation of motion and the normal modes

The Rouse model was the first microscopic approach to be used to describe single chain dynamics. It was first intended to model the motion of a polymer in a dilute fluid solution (Ref. 19).

The polymer is modelled according to the Gaussian chain, namely it is viewed as a chain of entropic springs (Gaussian segments) separated by beads (Fig.2.1). Each segment contains a number of monomeric units, large enough so that the distance between neighbouring beads is subject to Gaussian coiling. Therefore, a Rouse segment is much larger than the Kuhn length $b_k$. These segments are identical and have an average distance between the beads given by b. The beads are essentially points.

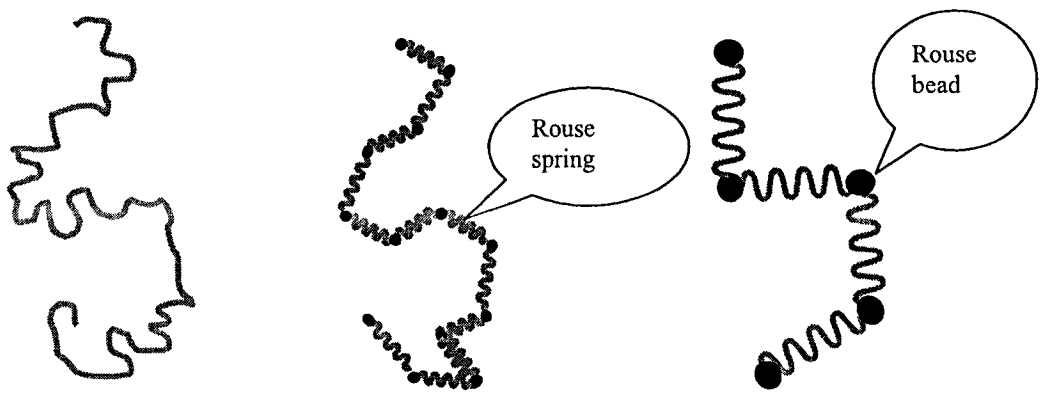


Fig. 2.1 The Rouse model for a linear polymer.

According to the Gaussian model, the harmonic spring potential energy for a system of N+1 beads can be written in the following form:

$$U = \frac{k}{2}\sum_{n=1}^{N}(\vec{R}_n - \vec{R}_{n-1})^2 \tag{2.14}$$

where $\vec{R}_0, \vec{R}_1, ..., \vec{R}_N$ are the positions of the beads and k is the spring elastic constant. The entropic character of the elastic constant is revealed by the equivalence between the geometric and the energetic distribution functions. Identifying the geometrical distribution

$$\begin{aligned}\Phi(\{r_n\}) &= \prod_{n=1}^{N}\left(\frac{3}{2\pi b^2}\right)^{3/2}\exp\left[-\frac{3r_n^2}{2b^2}\right] = \\ &= \left(\frac{3}{2\pi b^2}\right)^{3N/2}\exp\left[-\sum_{n=1}^{N}\frac{3(\vec{R}_n - \vec{R}_m)^2}{2b^2}\right]\end{aligned} \tag{2.15}$$

with the Boltzmann equilibrium function

$$\Phi \propto \exp\left(-\frac{U}{k_B T}\right) = \exp\left(-\frac{k}{2k_B T}\sum_{n=1}^{N}(\vec{R}_n - \vec{R}_{n-1})^2\right). \tag{2.16}$$

we obtain for the elastic spring constants

$$k = \frac{3k_B T}{b^2} \tag{2.17}$$

The Rouse theory can be easily presented using matrix algebra. The harmonic potential energy of the chain can be written as:

$$U = \frac{k}{2} R^T A R \tag{2.18}$$

where $R = (\vec{R}_0, \vec{R}_1, ..., \vec{R}_N)$ is the bead position row vector. Here A is a NxN symmetric force matrix describing the morphology of the chain, i.e. the way the beads are connected. It is usually called the connectivity matrix. For a linear chain it reads

$$A = \begin{bmatrix} 1 & -1 & & & & & \\ -1 & 2 & -1 & & & & \\ & -1 & 2 & -1 & & & \\ & & \cdot & \cdot & \cdot & & \\ & & & -1 & 2 & -1 & \\ & & & & -1 & 1 & \end{bmatrix}. \tag{2.19}$$

The model considers that each bead experiences three types of force: the elastic force between first neighbours, the friction force due to the viscous surroundings and the stochastic random force $\vec{f}(t)$ due to the Brownian motion of the fluid molecules around the chain. The force balance gives the so-called Langevin equation of motion:

$$\zeta \frac{\partial R(t)}{\partial t} = -kAR + F(t) \tag{2.20}$$

where $F(t) = (\vec{f}_0, \vec{f}_1, ..., \vec{f}_N)^T$ contains the random forces acting on each of the N+1 beads. These random forces are characterized by Gaussian distribution moments:

$$\begin{aligned} &\langle f_n(t)\rangle = 0, \\ &\langle f_{n\alpha}(t) f_{m\beta}(t')\rangle = 2\zeta k_B T \delta_{nm}\delta_{\alpha\beta}\delta(t-t') \quad (\alpha,\beta = x,y,z) \end{aligned} \tag{2.21}$$

The inertial forces are disregarded due to the overdamped character of the system. The hydrodynamic interactions between the beads are also neglected, together with the excluded volume interactions; these are in fact the most severe limitations of the model.

The form of the matrix A allows for diagonalization, that is the decoupling of the equations of motion. This will provide a new system with independent equations, each describing a normal mode of the chain. For this, we multiply the Langevin equation on the left with the inverse of a matrix V containing an orthonormal eigenvector of A in each column. When V multiplies A both sides, the result is a diagonal matrix D:

$$AV = VD \quad \text{or} \quad V^{-1}AV = D. \tag{2.22}$$

Then the Langevin equation becomes

$$\zeta \frac{\partial}{\partial t}\left(V^{-1}R\right) = -kV^{-1}AR + V^{-1}F. \tag{2.23}$$

If we name the product $V^{-1}R$ with X and $V^{-1}F$ with G, the equation becomes

$$\zeta \frac{\partial X(t)}{\partial t} = -kDX(t) + G \tag{2.24}$$

where

$$V^{-1}AR = DV^{-1}R = DX \tag{2.25}$$

The new variable X is a column vector containing the normal coordinates of the system $\{x_i\}$ and G contains the projections of the random force vectors on the A eigenspace. Clearly the entries in the diagonal matrix D are the eigenvalues $\{\lambda_i\}$ of A. For each row, Eq. 2.24 reads

$$\zeta \frac{\partial x_i(t)}{\partial t} = -k\lambda_i x_i(t) + g_i, \qquad i = 0,1,2,... \tag{2.26}$$

The time-dependent force $\vec{g}_i$ obeys the same conditions as $\vec{f}_i$:

$$\left\langle \vec{g}_i(t) \right\rangle = 0 \quad \text{and} \quad \left\langle \vec{g}_i(t)\vec{g}_j(t') \right\rangle = 2\zeta k_B T \delta_{ij}\delta(t-t'). \tag{2.27}$$

For a uniform linear chain, the eigenvalues $\lambda_i$ are given by the exact relation (Ref. 17):

$$\lambda_i = 4\sin^2\left(\frac{i\pi}{2(N+1)}\right), i = 0,1,2,... \tag{2.28}$$

The normal coordinates $x_i$ (usually called normal modes) are linear combinations of the position vectors $\vec{R}_i$, the factors being the components of the A eigenvectors:

$$\vec{x}_i(t) = \frac{1}{\sqrt{N+1}}\sum_{n=0}^{N}\cos\left(\frac{i\pi(n1)}{N+1}\right)\vec{R}_n(t) \quad i = 0,1,2,... \tag{2.29}$$

They are orthogonal.

Physically, the modes represent the internal conformation of the polymer on various length scales, except for the $0^{th}$ one, which is related to the position of the centre of the mass of the chain

$$\vec{R}_{cm} = \frac{1}{N+1}\sum_{n=0}^{N}\vec{R}_n = \frac{\vec{x}_0}{\sqrt{N+1}}. \tag{2.30}$$

The non-zero eigenvalues give the relaxation rates of the normal modes $x_i$, i=1, 2,…,N.

## 2.2.2 Chain dynamics. The autocorrelation functions

The physical observables of the system are fluctuating quantities. Statistically, the evolution of the system can be described by correlation functions of the observables. Focusing on the thesis subject, we refer here only to the dynamics of end-to-end vector.

With the normal coordinates, the end-to-end vector can be written as

$$\vec{h}(t) = \vec{R}_N(t) - \vec{R}_0(t) = -\frac{4}{\sqrt{N+1}}\sum_{i:odd}\vec{x}_i(t), \tag{2.31}$$

if $\vec{R}_n$ are expressed as function of $x_i$,

$$\vec{R}_n = \vec{x}_0 + \frac{2}{\sqrt{N+1}}\sum_{i=1}^{N}\vec{x}_i \cos\left(\frac{i\pi(n+1)}{N+1}\right) \tag{2.32}$$

The autoccorelation function of $\vec{h}$ is then a sum over the odd mode autocorrelation functions

$$C_h(t) = \left\langle \vec{h}(t)\cdot\vec{h}(0)\right\rangle = \frac{16}{N+1}\sum_{i:odd}\left\langle \vec{x}_i(t)\cdot\vec{x}_i(0)\right\rangle. \tag{2.33}$$

The following expressions hold for the mode autocorrelation functions (for a detailed derivation, see Ref. 2):

$$\left\langle \vec{x}_i(t)\cdot\vec{x}_i(0)\right\rangle = \frac{3k_BT}{\lambda_i k}\exp(-\lambda_i kt/\zeta). \tag{2.34}$$

This yields

$$C_h(t) = \frac{16}{N+1}\sum_{i:odd}\frac{3k_BT}{\lambda_i k}\exp\left(-\lambda_i kt/\zeta\right) \tag{2.35}$$

In the limit of very long chains, when Eq. 2.28 can be simplified to

$$\lambda_i \cong i^2 \lambda_1, \text{ with } \lambda_1 = \pi^2/(N+1)^2 \tag{2.36}$$

$C_h(t)$ becomes

$$\begin{aligned} C_h(t) &= \frac{48(N+1)k_BT}{k\pi^2} \sum_{i:odd} \frac{1}{i^2} \exp(-\lambda_i kt/\zeta) \\ &= const \cdot \sum_{i:odd} \frac{1}{i^2} \exp(-\lambda_i kt/\zeta) \end{aligned} \tag{2.37}$$

The expression above can be read as follows: the end-to-end vector relaxes as a superposition of exponentials with the characteristic times given by the mode relaxation times:

$$\tau_i = \zeta/\lambda_i k. \tag{2.38}$$

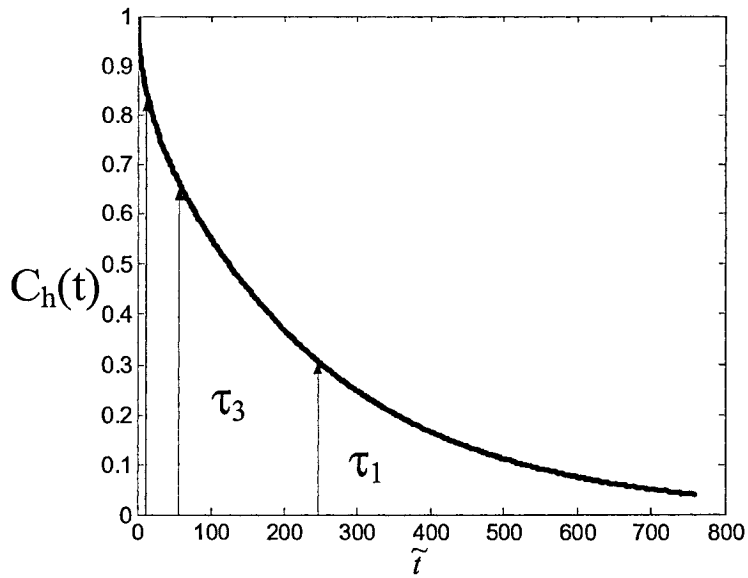


Fig. 2.2 The correlation function $C_h(t)$ is a multiexponential function. At large times it is nearly a simple exponential with $\tau_1$ the characteristic time.

At long times, the relaxation is essentially a single exponential with the characteristic time (for N large)

$$\tau_r = \tau_1 = \frac{\zeta(N+1)^2 b^2}{3\pi^2 k_B T}. \tag{2.39}$$

The first non-zero mode (i=1) mainly describes the change of a vector connecting the middle points of the two halves of the chain and is thus associated with the rotation of

the chain as a whole. Therefore, the characteristic time of the end-to-end vector correlation function is often named the rotational time.

The scaling relation $\tau_r \propto N^2$, however, does not agree with the experimental results for dilute solutions (in which case the mass exponent is 3/2), the situation actually first intended to be described by the model. But it turns out that the Rouse scaling describes very well melts where the hydrodynamic interactions are missing and the excluded volume interaction is screened.

The Rouse model has been modified to include the hydrodynamic and excluded volume interactions. Approximate solutions to these generalized Rouse models recover the proper scaling exponents, but exact solutions do not exist. Since our goal was to design a model that can be solved exactly even in the presence of disorder, we will be using the Rouse model presented here.

# Chapter 3

## Relaxation in complex systems: Non-exponential decay functions

### 3.1 Introduction: A stretched exponential fits many relaxation processes

For many disordered systems it is has been found that the relaxation fits a sub-unitary exponential function. Kohlrausch (Ref. 37) was the first (1847) to study the relaxation of complex electronic and molecular systems when he found that the decay of the residual charge on a glass jar was described by a stretched exponential function $\exp[-(t/\tau)^{\beta}]$. His result gave a value of 0.426 for the exponent $\beta$. Later, William and Watts (Ref. 38) used this function to describe dielectric relaxation in polymers. For almost 150 years now, there have been numerous experimental findings (Ref. 5) for which the Kohlrausch –William-Watt (KWW) function could fit the relaxation data successfully. But despite its quite general occurrence and its economical form (only one decisive sub-unitary parameter $\beta$) which entitles it to be seen as a natural universal law, there is no first principle theory yet that would relate rigorously the form of the decay function to the internal characteristics of the system which relaxes.

The common accepted features of the systems that relax in the KWW way is that they are in one or more of the following groups: disordered materials (contain site or local randomness), systems with strong many-body interactions, systems with non-linear mutual interactions, systems displaying fractal characteristics, or decay phenomena with rare events. Economic, social and biological laws were also fitted with this stretched exponential more successfully than with power laws or simple exponentials.

Among the physical systems, the most prone to a KWW relaxation were found to be the glassy systems. From the electronic material class these are, for example: spin glasses, metallic glasses (quasicrystals), semiconductor nanocrystallites, vortex glasses in high temperature semiconducting polymers. In the molecular group we mention polymers, electrolytes, Van der Waals supercooled liquids and glasses, network glasses and orientational glasses.

In the case of polymer solutions, remarkable work has been done for randomly branched polymers in a good solvent (Ref. 7-Ref. 9). A stretched exponential relaxation has been numerically found using Monte Carlo simulations. Here, the disorder factor materializes in the structure topology; a molecule is constructed from the connection of linear polymer chains, of various lengths, at branching sites that are randomly selected. The autocorrelation function, associated with the relaxation of the radius of gyration, displays a clear stretched exponential character.

In the field of biological polymers, we mention a numerical study of the dynamics of heteropolymeric chains, with application to protein folding (Ref. 13). The N parts of the chain describe the sequence of amino acids. The quantity under observation is the autocorrelation function of the chain energy. This model includes the harmonic potential of the bonds between nearest neighbors, the deterministic part of the potential in the usual Lennard–Jones form, and a quenched disorder term. The main interest of the work was to understand if the disordered nature of the chain is enough to explain the folding of a protein in a given final shape. The numerical results suggest that, in the folded phase, the system decays following a KWW function.

As for the theoretical investigations, either for molecular or electronic systems, the various attempts enter one of two scenarios (Ref. 14). The "heterogeneous" scenario (also known as the parallel relaxation mechanism) asserts that KWW relaxation emerges from a superposition of different simple exponential relaxations, when the characteristic times form a broad band distribution (Fig. 3.1),

$$e^{-(t/\tau)^{\beta}} = \int_0^{\infty} P(\tau) e^{-t/\tau} d\tau . \qquad (3.1)$$

The probability distribution of relaxation times, $P(\tau)$, is taken across different atoms, clusters or degrees of freedom.

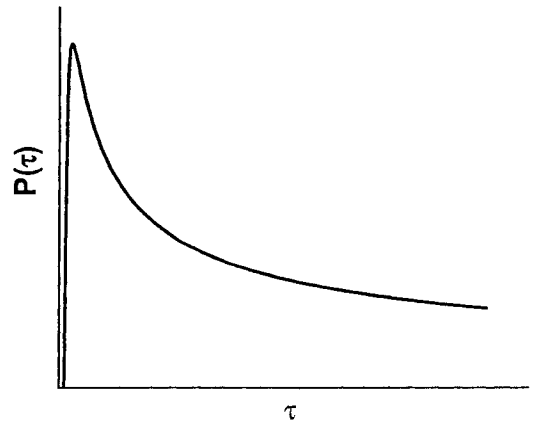


Fig.3.1. A continuous and broad distribution of charateristic times can lead to a KWW decay.

The underlying mathematical reason for this explanation originates from the following property: any monotonous function can be written as the Laplace transform of a non-negative function. This can be simply written using the relaxation rate variables, $\lambda=1/\tau$:

$$e^{-(t/T)^{\beta}} = e^{-(\Lambda t)^{\beta}} = \int_0^{\infty} p(\lambda)\exp(-\lambda t)d\lambda = L(p(\lambda)) \tag{3.2}$$

where L is the Laplace transform:

$$L[f(x)] = \int_0^{\infty} f(x)\exp(-xt)dx \tag{3.3}$$

With this, at least in principle, the distribution of relaxation rates (or characteristic times) can be found via the inverse Laplace transform

$$p(\lambda) = L^{-1}\left(e^{-(\Lambda t)^{\beta}}\right). \tag{3.4}$$

However, an analytical solution exists only for $\beta = 1$ and $\beta = 1/2$. For the latter, it gives

$$p(\lambda, \beta = 1/2) = \frac{1}{\lambda^{3/2}}\exp\left(-\frac{c}{\lambda}\right) \tag{3.5}$$

For other values of $\beta$, the rate distribution must be obtained numerically.

But the above scenario is rather arbitrary from the microscopic point of view. This is not in favor to the claimed universality of the KWW law, revealed by experimental data. Therefore, many authors find more justifiable the second scenario. This considers

that all the particles in the system relax identically but in an intrinsically non-exponential way. Chronologically, this so-called "homogeneous" scenario was developed more recently than the "heterogeneous" scenario.

In the following sections of this chapter, we will review some of the most relevant proposed theoretical models for KWW relaxation. These models were designed to describe charge relaxation, the relaxation of spin glasses and the rheological behavior of polydisperse polymeric melts. A possible unifying theory is discussed in section 3.5, together with example of the entangled monodisperse polymer system.

## 3.2 A model for parallel relaxation (charge relaxation)

Forster was the first to develop a model for a parallel relaxation mechanism for the KWW decay (Ref. 12). It was formulated to explain the excitation transfer from a donor to static defects in various condensed materials. This model can actually describe the charge relaxation in amorphous semiconductors where the excitons (donors) diffuse and recombine non-radiatively at defect sites. The relaxation function is the probability that the exciton still exists when a defect is placed at $R_i$ (Fig. 3.2)

$$q_i(t) = \exp(-t\lambda(R_i)), \tag{3.6}$$

where $\lambda(R_i)$ is the relaxation rate as a function of the distance to the $i^{th}$ donor (see Fig.3.2). For many

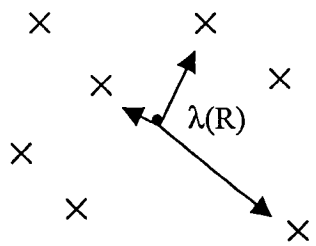


Fig.3.2. A donor (•) can transfer its energy via parallel channels to a configuration of defects (x). The transition rate to site R is denoted by λ(R).

defects (excluding the donor site) one has

$$q(t)=\prod_{i=1}{}'\exp(-t\lambda(R_i)). \tag{3.7}$$

If the probability that a site is occupied by a defect is p, the equation above becomes

$$q(t)=\prod_{i=1}{}'[1-p+p\exp(-t\lambda(R_i))]. \tag{3.8}$$

The probability p has to be small enough to be appropriate for the distribution of defects and consequently, $q(t)$ can be well approximated by the following expression:

$$q(t)\approx\exp\left(-p\sum_i{}'[1-\exp(-t\lambda(R_i))]\right). \tag{3.9}$$

The sum can be transformed into an integral by introducing the site density function,

$$\rho(R)=\sum_i{}'\delta(R-R_i). \tag{3.10}$$

Hence,

$$q(t)\approx\exp\left(-p\int_0^\infty\rho(R)\left[1-\exp\left(-t\lambda(R)\right)\right]dR\right). \tag{3.11}$$

The form of the relaxation rate $\lambda(R)$ depends on the type of interaction between the donor and the defects. For isotropic interactions, it has been shown that $\lambda(R)=aR^{-s}$ (a and s are material related constants). After some integral calculus approximations, a KWW type relaxation is obtained:

$$q(t)\approx\exp\left[-(t/\tau)^{\beta}\right] \tag{3.12}$$

where $\beta=3/s$ ($\rho(R)$ was taken to be a constant). In Forester's energy transfer problem $s\geq6$ and $\beta\leq1/2$.

## 3.3 A hierarchically constrained dynamic model (spin glasses)

This model considers that the relaxation is non-exponential in nature because it proceeds hierarchically (Ref. 10). This situation applies when smaller subsystems must be relaxed to a certain extent in order to initiate the relaxation of larger subsystems. Palmer et al. proposed the first detailed model that relies on this serial aspect of

relaxation. Intended for a glassy system, it comprises hierarchies, constraints and dynamics as three features driving to non-exponential relaxation. The same Eq. 3.1 is used, but now the $\tau_n$'s and thus the $p(\tau_n)$'s are not independent variables anymore.

The system degrees of freedom, here Ising spins, are divided into a sequence of levels n=0,1,2,... Each spin in level n is free to change its state, after a certain condition in the previous level is met. For instance, a change in the n+1 level state occurs when $\mu_n$ spins in the $n^{th}$ level reach one of their $2^{\mu_n}$ possible states, i.e.

$$\tau_{n+1} = f(\tau_n, \mu_n) = 2^{\mu_n}\tau_n \tag{3.13}$$

The relaxation for each spin is taken to be exponential and the characteristic time is the same for all $\mu_n$ spins in level n. Therefore, the correlation function is written as a summation of exponential functions, over all levels,

$$q(t) = \sum_{n=0}^{\infty} w_n \exp(-t/\tau_n) \tag{3.14}$$

where the weighting factor is $w_n=N_n/N$ and N is the total number of spins. The relaxation time $\tau_n$ can be obtained from Eq. 3.13:

$$\tau_n = \tau_0 \exp\left(\sum_{k=0}^{n-1} \mu_k \ln 2\right). \tag{3.15}$$

The possible choices for $\mu_n$ are constrained by the convergence of the sum above, in order to assure finite values for $\tau_n$. At large times, i.e. when $t>>\tau_{max}$ ($\tau_{max}=\lim_{n\to\infty}\tau_n$), Eq. 3.14 will necessarily give a pure exponential relaxation. Of course the weights $w_n$ must decrease with n to keep $N = \sum_{n=0}^{\infty} N_n$ finite.

Most of the possible choices for these two parameters lead to power law relaxation. In accordance with our goal, we mention here the case that gives a stretched exponential relaxation. This occurs when $\mu_n=\mu_0/n^p$, and $N_{n+1}=N_n/\lambda$, $\lambda>1$. The characteristic times then become

$$\tau_n = \tau_0 \exp\left(\mu_0 \ln 2 \sum_{k=1}^{n} k^{-p}\right) \underset{p=1}{\approx} \tau_0 n^{\mu_0 \ln 2}. \tag{3.16}$$

Replacing the sum with an integral in Eq. 3.14 and using the above expression one gets

$$q(t) = w_o \int_0^\infty \lambda^{-n} \exp\left(-\frac{t}{\tau_0 n^{\mu_0 \ln 2}}\right) dn. \tag{3.17}$$

This integral can be approximated by the method of steepest descent and gives

$$q(t) = c_1 e^{-(c_2 t)^\beta} \text{ with } \beta = 1/(1+\mu_0 \ln 2), \tag{3.18}$$

namely, a KWW function.

## 3.4 Stretched exponential relaxation in a polydisperse system of non-interacting linear polymers

Here we present a recent, simple theoretical justification for the sub-unitary exponential relaxation in a polymer melt (Ref. 20). The system is made up of linear polymers with length polydispersity. The method can be used for both Rouse dynamics and reptation dynamics. Because there are no interchain interactions, this theory belongs to the parallel relaxation mechanism scenario that explains the non-exponential decay through a broad distribution of relaxation rates (or characteristic times).

The decay function $\Phi(t)$ is, accordingly, a sum over the individual exponential decays, weighted by the distribution of relaxation rates f,

$$\Phi(t) = \int_0^\infty df W(f) e^{-ft} \quad . \tag{3.19}$$

The integration variable f is taken over all chains in the melt, but only the smallest Rousean frequency (the longest relaxation time) is considered for each chain, i.e.

$$f(N) = \frac{\lambda_1 k}{\zeta} = \frac{\pi^2 k}{\zeta N^2} = \frac{1}{\tau_0} N^{-2}. \tag{3.20}$$

where $\tau_0$ is the characteristic time for a unit size chain.

Typical polymerization conditions allow for the use of a Boltzmann type distribution for the chain lengths (or the polymerization index) N (Ref. 27),

$$P(N) = C(N) \exp(-N/\overline{N}), \qquad (N > \overline{N}) \tag{3.21}$$

where C(N) is a power law, hence slowly varying function, and $\overline{N}$ is the average chain size. The distribution function W(f) can now be found, if one converts the N distribution into a distribution for the relaxation frequencies,

$$W(f)|df| = P(N)dN \ . \tag{3.22}$$

We get

$$W(f) = A(f)\exp\left(-\frac{1}{\overline{N}}\left(\frac{1}{f\tau_0}\right)^{1/2}\right), \tag{3.23}$$

where the factor A(f) includes all the power law functions:

$$A(f) = C\left(1/(f\tau_0)^{1/2}\right)\frac{1}{2\tau_0^{1/2}f^{3/2}}. \tag{3.24}$$

We note here that the f-dependence of the distribution function W(f), found in Ref. 20, is similar to the expression of the analytical solution for the probability distribution of the relaxation rates in the "heterogeneous" scenario (see Eq. 3.5),

$$p(\lambda) = \frac{1}{\lambda^{3/2}}\exp\left(-\frac{c}{\lambda^x}\right) \tag{3.25}$$

with x=1/2. The form of W(f), as a sharp descending function at small f, together with the factor $e^{-ft}$, gives a one-maximum type function for the integrand in (3.19). The dominant exponential factor

$$\exp[-S(f,t)] \equiv \exp\left[-ft - \left(\frac{f_0}{f}\right)^{1/2}\right], \tag{3.26}$$

with

$$f_0 = \frac{1}{\overline{N}^2\tau_0}, \tag{3.27}$$

will thus be preserved after integration. Considering only the minimum of S with respect to f, that is, only the f values along the curve

$$f = f^*(t) = \frac{f_0^{1/3}}{2^{2/3}}\frac{1}{t^{2/3}} \tag{3.28}$$

the asymptotic relaxation function becomes

$$\Phi(t) = B(t)\exp\left[-(\hat{f}t)^{1/3}\right]. \tag{3.29}$$

The factor B(t) is a power law function and

$$\hat{f} = 6.75f_0. \tag{3.30}$$

In this simple way, a stretched exponential function (β=1/3) is found for the structure relaxation function Φ(t). The central point in the above derivation is the

presence of the exponential distribution of the polymerization index N, that leads to a sharp decreasing functional form of W(f) at small f. The exponent $\beta$ turns out to be sensitive to the presence or absence of entanglements; when the smallest rate f is replaced by its value for reptation dynamics,

$$f(N) = \frac{1}{\tau_0} N_e N^{-3} \qquad (N >> N_e) \tag{3.31}$$

the method above gives $\beta = 1/4$. Here $N_e$ is the distance (in chain units) between the entanglements. This elegant theory suggests that stretched exponentials might be quite general in polymeric systems since polydispersity is extremely common.

## 3.5 System size dependence of relaxational processes

The mathematical reasons for which the two previous models lead to a stretched exponential relaxation are conceptually equivalent. Both equations 3.17 and 3.19 can be written in a general form as:

$$q(t) = \int_0^\infty \exp(-an^\alpha) \exp(-\frac{bt}{n^\gamma}) dn \tag{3.32}$$

with $\alpha$=1, $\gamma$=$\mu_0$ln2 for the hierarchical model, and $\alpha$=-1 ,$\gamma$=1/2 for the polydisperse polymer system. The first exponential is the probability p(n) that state n is occupied, whereas the second exponential is the relaxation function for state n, Q(n,t). These integrals were evaluated for large t by the method of steepest descend, i.e. the integral was approximated with the integrant's maximum value. For the above expression, this implies finding the value $n^*$ for which the exponent $-an^\alpha - bt/n^\gamma$ is maximum and then using it as the integrant. Solving for $n^*$ we get

$$n^* = \left(\frac{\gamma bt}{\alpha a}\right)^{\frac{1}{\alpha+\gamma}} \tag{3.33}$$

and so

$$q(t) \cong \exp(-(t/\tau)^\beta). \tag{3.34}$$

This is a stretched exponential function with the parameters $\beta=\alpha/(\alpha+\gamma)<1$ and $\tau=(\alpha/b\gamma)a^{-\gamma/\alpha}[\gamma/(\gamma+\alpha)]^{1+\gamma/\alpha}$. So far, for both systems the ensemble size was considered to be infinite (thermodynamic limit) through the [0, ∞] settings for the integral limits. However, for many practical situations the stretched exponential regime has a limited duration, after which a simple exponential decay sets in. It has been shown (Ref. 34) that for this model, this limitation is due to the finite size of the system. In this case, the relaxation function is actually the average relaxation over the N elements of the system,

$$q(t)=\frac{1}{N}\sum_{\{n\}}m(n)Q(n,t) \tag{3.35}$$

where the sum is over all possible states n, and m(n) is the number of elements in state n, with $\sum_{\{n\}}m(n)=N$. When $N\to\infty$, all states are occupied and $m(n)/N\to p(n)$ such that q(t) can be written in the integral form of Eq. 3.35. But when N has a finite value, the integral upper limit has to be replaced by a maximum value $n_{max}$, i.e.

$$q(t)=\int_0^{n_{max}}p(n)Q(n,t)dn. \tag{3.36}$$

The quantity $n_{max}$ is a system size variable and it can be estimated by the following condition: the $n_{max}$ state exists only if it contains at least one element, i.e. it exist only if $N\cdot\exp(-an^{\alpha})\sim 1$. This yields

$$n_{max}\cong\left(\frac{\ln N}{a}\right)^{1/\alpha} \tag{3.37}$$

If the maximum of the integrant occurs well before $n_{max}$, i.e. $n^{*}<<n_{max}$, the relaxation proceeds in a stretched exponential form for all times. If, on the contrary, $n^{*}>>n_{max}$, the main contribution to Eq. 3.36 comes from the $n_{max}$ term,

$$q(t)\cong q(0)\exp\left(-\frac{bt}{n_{max}^{\gamma}}\right). \tag{3.38}$$

Thus, the system relaxes in a simple exponential manner for times $t>t_x$. The crosssover time from a stretched exponential to a simple exponential can be estimated from the condition $n^{*}=n_{max}$. This yields

$$t_x\cong\frac{\alpha a}{\gamma b}\left(\frac{\ln N}{a}\right)^{1+\gamma/\alpha}. \tag{3.39}$$

Identifying the logarithmic size dependence of the crossover time in experiments may provide support to the theories claiming that the observed stretched exponential is due to the competition of two exponential processes.

## 3.6 The coupling model. Chaotic dynamics as a central explanation for relaxation in complex systems

The aim of this section is to briefly present one of the first theoretical attempt intended to provide a universal explanation for the sub-unitary exponential relaxation in disordered systems (Ref. 5). The universality of the disordered system relaxation pattern, established either experimentally or by computer simulations, naturally requires a general theoretical foundation. Various systems are included here, for example densely packed polymer chains, viscous small molecule liquids, ionic glasses with a high density of mobile ions, etc. Some typical systems are given in Table 3.1. These systems have relaxing units that are strongly packed together so that they are strongly correlated. For this reason, they are collectively called complex correlated systems. Their relaxation is therefore cooperative. Well-established models exist only for low concentrations, when the relaxation of the constituents becomes uncorrelated. Here we mention the Rouse model for the relaxation of chains in dilute solutions or the ion conductivity relaxation in alkali oxide glasses within the limit of low ion concentration. Otherwise, solving the dynamics of such systems is a very complicated, if not an impossible task, due to the correlated nature of the process. So far there is no known method for a complete solution.

The correlation between the relaxing species is caused by their mutual interactions. Usually, these are nonlinear pair potentials such as the Lennard-Jones potential, the Morse potential and the screened Coulomb interaction. From a statistical point of view, these examples are interacting many body systems and their relaxation is an irreversible process.

Table 3.1. Features of some typical correlated systems.

| Correlated system (CS) | Relaxing species | Nature of mutual interactions |
|---|---|---|
| Glass-forming viscous liquids | Structural units or units forming a cooperative rearrangement regions (CRR) | Inter-molecular interactions between the structural units or between the CRR's |
| Monodisperse linear polymer melts (terminal relaxation) | A single chain | Entanglement interactions between polymer chains (non-crossability of long chains) |
| Ionic conductors (vitreous): $(Li_2O)_x(B_2O_3)_{1-x},O_3$ Crystalline $Na\beta Al_2$ | An ion in a glassy matrix | Screened Coulomb interactions between the ions in the glassy matrix |

Ngai (Ref. 5, chapter 2) considers that the relaxation of complex systems has to be studied using the phase space dynamic methods. The nonlinear and nonintegrable character of the Hamiltonians translates the motion in the phase space into chaotic dynamics. Here, similar patterns occur, irrespective of the details of the potentials. Therefore, it seems to be appropriate to construct a theory of relaxation in complex systems based on the physics of chaos in nonintegrable conservative systems.

The first attempt to model the structure of the phase space assumed that it has a fractal characteristic. This assumption makes possible a solution via diffusion in fractal topologies, diffusion that it is known to be anomalous,

$$\left\langle r^2(t)\right\rangle \cong t^{2/\tilde{d}} \tag{3.40}$$

where the anomalous diffusion exponent $\tilde{d} > 2$. The physical picture proposed for the relaxation is the following: at sufficiently short times, the mutual interaction between units has no effect on the dynamics, and hence they relax independently with a relaxation rate $\lambda_0$. The time span for this independent relaxation process $t_c=1/\omega_c$, called the crossover time, depends on the nature and strength of the mutual interactions. The existence of such a $t_c$, which is temperature independent, has been confirmed experimentally and by computer simulations. It was found, for example, that for monodisperse linear polymer melts $t_c$ ~10-100 psec. After a time $t_c$, the interactions slow

down the relaxation rate because of the diffusion through a fractal chaotic phase space. Quantitatively we thus have:

$$\lambda(t)=\begin{cases}\lambda_0 & t<t_c\\ \lambda_0(\omega_c t)^{-n} & t>t_c\end{cases}. \tag{3.41}$$

Writing the average square displacement as 2Dt in Eq. 3.40 and using the time inverse proportionality of the diffusion coefficient $D\sim 1/\tau\sim\lambda$, we obtain

$$n=1-2/\tilde{d}. \tag{3.42}$$

The rate exponent is thus directly related to the anomalous exponent $\tilde{d}$. Consequently the relaxation function is ($\tau_0=1/\lambda_0$)

$$q(t)=\begin{cases}\exp-(t/\tau_0) & t<t_c,\\ \exp-(t/\tau^*)^{(1-n)} & t>t_c,\end{cases} \tag{3.43}$$

with the effective relaxation time,

$$\tau^*=\left[\omega_c^n\tau_0\right]^{1/(1-n)}. \tag{3.44}$$

The exponent n is called the coupling parameter from a reason that will be clear immediately. First we notice that the expression obtained for the relaxation function (Eq. 3.43) is a consequence of the form of the relaxation rates (Eq. 3.41). Since $\tilde{d}\geq 2$, n lies between zero and one. It is zero when there are no mutual interactions among the constituents and, as a consequence, the phase space is then Euclidean ($\tilde{d}=2$). In this case the relaxation is exponential at all times ($t_c\rightarrow\infty$) . On the other hand, the more intense the interactions, the more chaotic the phase space becomes. The anomalous diffusion coefficient $\tilde{d}$ will increase monotonically with interaction strength and consequently n will increase too. In such cases, the relaxation takes the form of a stretched exponential with the exponent (1-n)<1.

The merit of the above derivation rests in the simplicity of its deductions. It was indeed confirmed experimentally and by computer simulations in a great number of situations. According to the physical interpretation, the $t_c$ values have to be somewhere between molecular vibrations and molecular dynamics characteristic times. Indeed, the experimental results gave realistic values for $t_c$, when estimated through the effective relaxation time $\tau^*$ from Eq. 3.36. Its shortcoming is the lack of transport details in the

phase space. As before, in agreement with our goals here, we will describe a more refined model that includes some more details about the transport in phase space without entering into mathematical details (see Ref. 5, chapter 2).

Let us consider the situation of an entangled monodisperse linear polymer chain system, although the result is also valid for other physical systems. Accordingly, the nonlinear part $H_1$ of the total Hamiltonian, $H=H_0+H_1$, may originate from the Lennard – Jones potential. The crossover time for the occurrence of the dynamical correlation between the polymer chains is associated with the onset of island configuration in the phase space. These islands slow down the flowing in the phase space and it has been shown (Ref. 36) that the dynamic effective friction coefficient that can model this slowing down has the following time dependence

$$\zeta(t) \propto t^{n_i}, \qquad 0 < n_i < 1. \tag{3.45}$$

As we already know, in the absence of correlation (i.e., before time $t_c$), the dynamics of the polymeric chain can be represented by the Langevin equation (see section 2.2)

$$\zeta_0 \frac{dx_i}{dt} = -\lambda_i x_i + f_i. \tag{3.46}$$

The relaxation of the $i^{th}$ normal coordinate is then a simple exponential function,

$$\langle x_i(t)x_i(0)\rangle = \langle x_i(0)x_i(0)\rangle \exp(-t/\tau_{0i}). \tag{3.47}$$

For each Rousean mode, the friction coefficient has to be a continuous function of time:

$$\zeta(t) = \zeta_0 (t/t_c)^{n_i}, \quad t > t_c. \tag{3.48}$$

With this, the Langevin equation in the dynamically correlated regime ($t>t_c$) is written:

$$\zeta_0 (t/t_c)^{n_i} \frac{dx_i(t)}{dt} = -\lambda_i x_i(t) + f_i. \tag{3.49}$$

Solving the above equation gives the correlation function of the i'th normal mode,

$$\langle x_i(t)x_i(0)\rangle = \langle x_i(0)x_i(0)\rangle \exp\left(-(t/\tau^*)^{1-n_i}\right), \tag{3.50}$$

a stretched exponential function. In this way, each Rouse mode relaxes intrinsically in a non-exponential manner (KWW relaxation). The effective relaxation time is accordingly,

$$\tau_i^* = \left[(1-n)t_c^{-n}\tau_{0i}\right]^{1/(1-n_i)}, \tag{3.51}$$

a function of the independent single relaxation time $\tau_{0i}$.

In conclusion, we briefly showed how the chaotic dynamic of correlated systems may provide a theoretical explanation for relaxation in complex systems. The interpretation is the modification of the flow in the phase space due to the formation of islands of chains (self-similar island-around-island structures). With this, an interpretation for the stretched exponential $\beta$ coefficient is also obtained, as a measure of the mutual intensity of the interactions between the system constituents. We note here the occurrence of a conceptual contradiction when the friction coefficient $\zeta(t)$ is introduced in a nonintegrable conservative system. The above derivation goal is to offer a plausible explanation for the particular type of relaxation in these systems. The irreversibility of the relaxation processes poses important problems when solving the dynamics of a nonintegrable conservative system, which is usually reversible. Therefore the shortcomings of this derivation can be absolved in the light of the immense difficulties of introducing irreversibility into already complicated dynamics in phase space.

We should mention that the coupling model, as was presented here, applies strictly to the relaxation of macroscopic variables like enthalpy, stress, dielectric polarization, and density fluctuations. The relaxation is viewed as an average over all individual relaxing units. A heterogeneous character is implied for the relaxation of the individual units as a result of the microscopic picture of the correlated systems. This aspect was indeed proved experimentally, by NMR experiments.

## 3.7 Stretched exponentials and the Rouse model

In order to understand the non-exponential relaxation phenomena, we investigate whether a macromolecule modeled as a Rouse chain can relax in a KWW way. The absence of hydrodynamic and excluded volume interactions, together with the use of harmonic springs, eliminate from the beginning the coupling between the Rousean modes, the relaxing units in this case. The structural hierarchy is also absent (section 3.3). Moreover, a Rouse system has no entanglements, and so, the coupling model (section 3.5) is not applicable in a dilute solution. However, there is one more case that could potentially lead to a non-exponential relaxation - the heterogeneuous scenario or the

broadening of the distribution of characteristic individual times (Eqs. 3.2-3.4). Disorder, either intrinsic or extrinsic, might provide the required conditions for a KWW decay. Moreover, this picture would be justified by the natural polydispersity of real polymers. Intrinsic disorder can be either in the springs or in the friction coefficient. Can we have continuous spectra (hence proper Laplace transforms) with a single disordered chain? Does the relaxation of an ensemble of disordered chains follow a KWW function? Is the competition between two exponential processes a relevant mechanism for an ensemble of disordered chains? In the next chapter we try to answer these questions for an exactly solvable model that we have constructed in order to include a controlled amount of disorder.

# Chapter 4

## The equilibrium relaxation of non-uniform Rouse chains

Polymers can have structural polydispersity that involves disorder in various aspects. The aim of this chapter is to study the effect of one type of intrachain disorder on the relaxation behaviour of linear polymer chains. We investigate whether this type of intramolecular disorder modifies the long time exponential relaxation of the polymeric chain. In the light of various theoretical and experimental results (the most relevant were described in chapter 3) we compare the obtained decay functions with the stretched exponential relaxation.

As we have already seen, the Rouse model predicts a multiexponential decay for the configurational relaxation of polymeric chains. Here, the polymer dynamics is exactly solved with the aid of several simplifying assumptions regarding the solvent environment and the internal structure of the polymer. The most important assumptions concern the fact that the Rouse model neglects both the excluded volume interactions and the hydrodynamic ones. It is also limited by the length of the chain units – very rapid relaxation processes might occur on length scales shorter than the Rouse segment. Finally, the Rouse model assumes that the bead friction coefficient $\zeta$ and the elastic constant of the units, k, are constants along the chain. The impact of a non-uniform value of $\zeta$ on the mechanical properties such as the reduced storage and the loss moduli of polymeric networks was studied in the case of a regular but alternating sequence of beads (Ref. 35). In this chapter we focus on the influence of k heterogeneity on the conformational relaxational process. We modify the original Rouse model to include different types of polydispersity.

The type of disorder we consider is inspired from the random multiblock linear copolymer with a stochastic arrangement of monomer blocks along the chain. Copolymers are obtained by the common polymerization (or polycondensation) of

different monomeric substances. We can design a possible arrangement for a random block copolymer as

AFCCADAB...DCBCBBAD,

where each letter is a block formed by a random combination of two or more monomers, $[(a)_{nA}(b)_{nB}...]$. The degree of randomness can vary from a nearly ordered block copolymer, up to a completely random sequence of monomers, a situation found mostly in biopolymers. For example, most proteins can be well described as essentially random sequences of hydrophobic and hydrophilic amino-acid residues.

Let the total number of monomers in each block be the same ($n=n_A+n_B=$ constant) and the length of each block to be long enough (n~20-30 may suffice) in order to obey a Gaussian probability function. Because of the random values of the ratio $f= n_A/n_B$, the elastic constants of the spring units vary and a certain value can be assigned to each block in the chain. The heterogeinity of the chain then arises from the polydispersity of the

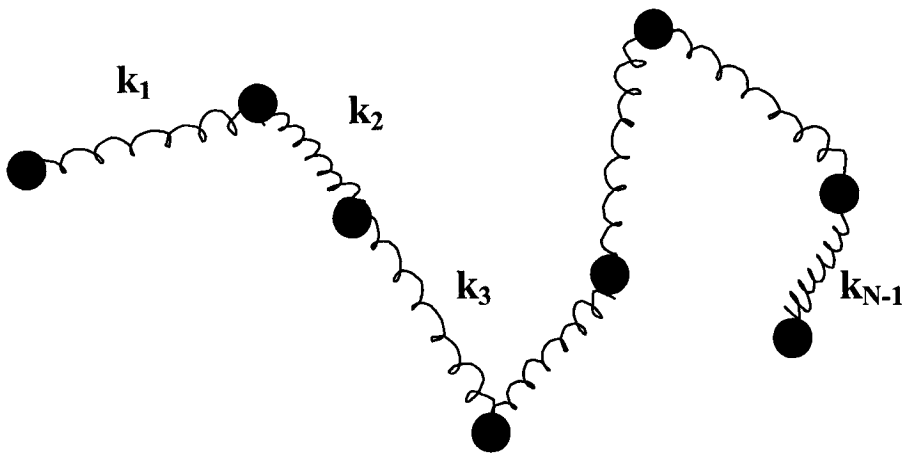


Fig. 4.1 The non-uniform Rouse chain with N beads and N-1 springs.

entropic springs of the Rouse units (Fig. 4.1). The elastic constants $\{k_i\}$ are related to the physical parameters (the average size of the segment, $b_n$, and the temperature T), via the necessary equivalence of the two types of chain description, the Gaussian and Boltzmann distribution functions:

$$\Psi\left(\{\vec{R}_n\}\right)=\prod_{n=1}^{N}\left(\frac{3}{2\pi b_n^2}\right)^{3/2}\exp\left[-\frac{3\left(\vec{R}_n-\vec{R}_{n-1}\right)^2}{2b_n^2}\right]$$
$$\propto \exp\left[-\frac{1}{2k_BT}\sum_{n=1}^{N}k_n\left(\vec{R}_n-\vec{R}_{n-1}\right)^2\right] \tag{4.1}$$

where $\vec{R}_i$ is the position of bead i. We thus identify the local harmonic spring constants as

$$k_n=\frac{3k_BT}{b_n^2} \tag{4.2}$$

We see that the variation of the average (in a mean square sense) equilibrium length, $b_n$, can come from the variation in the local stiffness of the chain due to different values of the compositional fraction $f=n_A/n_B$. A minimum possible size for the units (e.g., for one segment $n_A+n_B=20$) does exhibit this variation; meanwhile, one then avoids the loss of information about short length scale relaxation. We assume, for simplicity, that the monomer friction coefficients are the same $\zeta_A=\zeta_B$.

We are interested in the influence of the elastic constant heterogeneity upon the dynamics of the chain. We test several probability distributions for $k_n$ and analyze numerically the response in the form of the eigenvalue (frequency) spectra $H(\lambda)$ for each case. We then examine the characteristics of the spectra by investigating the distribution of eigenvalues. The relative arrangement of the individual frequencies is crucial for the dynamic response of the system. Then, we study the autocorrelation functions of the end-to-end distance constructed with the spectra. Given the numerous results obtained for the relaxation of disordered systems, we may expect a non-exponential form of the decay function, at long times. We thus compare our results for the relaxation functions with the Kohlrausch-Williams-Watts (KWW) stretched exponential $\exp[-(t/\tau)^{\beta}]$, the most widely used fitting function for the study of relaxation data in systems with disorder.

One of the questions that arise here is whether the non-exponential behaviour is indeed an intrinsic property of the randomness. If so, it should appear even in simple systems such this linear Rouse chain. Therefore, we first analyse the dynamic behaviour of a single random chain, followed by the study of a non-interacting ensemble of such polymers. Our study is semi-quantitative and it focuses on general features.

## 4.1 The Langevin equation for a random chain

The central quantity that determines the particular motion of the polymer chain is the connectivity matrix A. As we mentioned in chapter 2, A describes the topology of the N bead macromolecule and it enters the Langevin equation of motion in the following way:

$$\zeta \frac{d\vec{R}}{dt} = -kA\vec{R} + \vec{F}(t). \tag{4.3}$$

The diagonalization of A solves the eigenvalue problem for such a system. The eigenvalues are directly related to the frequencies of the chain normal modes. For the classic Rouse chain, i.e. uniform elastic spring constants, the spectrum is discrete (see Eq. 2.28) and the relaxation is simply a sum of exponentials with characteristic times given by Eq. 2.33.

For a chain with an elastic constant polydispersity, the matrix A will contain not only the topology information but also the relative strengths of the springs. In this case, we can formally write the Langevin equation,

$$\zeta \frac{d\vec{R}}{dt} = -k_{av} A_{\{\kappa_i\}} \vec{R} + \vec{F}(t) \tag{4.4}$$

where $k_{av}$ is the average elastic constant

$$k_{av} = \int_0^\infty kP(k)dk. \tag{4.5}$$

and

$$\kappa_i = \frac{k_i}{k_{av}} \tag{4.6}$$

are the reduced spring elastic constants. The matrix A then reads:

$$A_{\{\kappa_i\}} \equiv \begin{bmatrix} \kappa_1 & -\kappa_1 & & & \\ -\kappa_1 & \kappa_1+\kappa_2 & -\kappa_2 & & \\ & -\kappa_2 & \kappa_1+\kappa_3 & -\kappa_3 & \dots \\ & & \dots & \dots & -\kappa_N \\ & & & -\kappa_N & \kappa_N \end{bmatrix} \tag{4.7}$$

The spring constants $\kappa_i$ thus follow mean one probability distributions

$$1 = \int_0^\infty \kappa\, p(\kappa) d\kappa \tag{4.8}$$

where

$$p(\kappa) = P(k) k_{av} . \tag{4.9}$$

The eigenvalues of the new matrix $A_{\{\kappa i\}}$ are very complicated functions with no regular forms. However, the spectrum is still discrete, a general result in linear algebra. In the light of this, in the next sections, our study focuses on the numerical investigation of $A_{\{\kappa i\}}$ spectra, when different types of distributions $p\{\kappa\}$ are chosen.

## 4.2 Four types of distributions for the spring elastic constants

The normalized probability distributions we chose for $\kappa_i$ are the uniform, the dichotomous, the anomalous and the exponential distributions (Fig. 4.2). They represent different situations. The uniform distribution

$$p_u(\kappa) = \begin{cases} \dfrac{1}{2\Delta\kappa}, & \kappa \in [1-\Delta\kappa, 1+\Delta\kappa] \\ 0, & otherwise \end{cases}, \tag{4.10.a}$$

$$E_u[\kappa] = 1 \ , \ \sigma_u = \frac{\Delta\kappa}{\sqrt{12}} \ , \tag{4.10.b}$$

is a simple alternative to the Gaussian distribution, the most frequently used in physics. It is convenient since it doesn't contain negative elastic constants. The dichotomous probability distribution

$$p_d(\kappa) = \frac{1}{2}\big(\delta(\kappa-(1-\Delta\kappa)) + \delta(\kappa-(1+\Delta\kappa))\big), \tag{4.11a}$$

$$E_d[\kappa] = 1 \, , \ \sigma_d = \Delta\kappa \tag{4.11b}$$

only allows the values: $\kappa=1+\Delta\kappa$ and $\kappa=1-\Delta\kappa$. This creates a random diblock copolymer structure and, in the limit $\Delta\kappa \to 1$, the system is a mixture of stiff and very weak springs. Because of the symmetry, $\Delta\kappa$ cannot exceed the value of one in these first two cases. This is why we also introduce our anomalous distribution

$$p_a(\kappa) = \frac{2}{\pi\left(\kappa^3 + \frac{1}{4\kappa}\right)} \tag{4.12a}$$

$$E_a[\kappa] = 1,\ \sigma_a = \infty. \tag{4.12b}$$

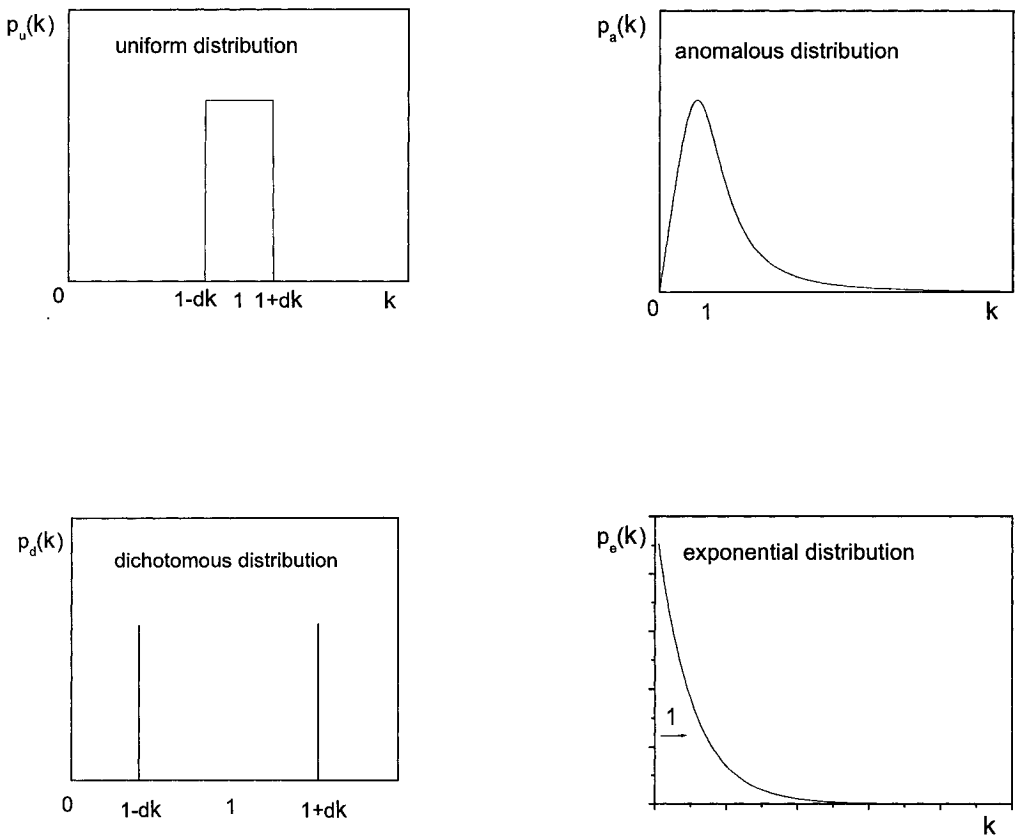


Fig. 4.2 The four types of distributions of the reduced elastic constants κ of our disordered Rouse chains.

The infinite variance is due to the slow algebric ($\sim\kappa^{-3}$) decay of the distribution for high values of the elastic constants. Finally, the reduced elastic constants are distributed according to the exponential distribution

$$p_e(\kappa) = \exp(-\kappa) \tag{4.13a}$$

with

$$E_e[\kappa]=1,\ \ \sigma_\kappa=1. \qquad (4.13b)$$

In this case we have a large probability of getting very low κ values (κ<<1).

## 4.3 The eigenvalue spectra for random chains

An overall view of the eigenvalue distributions can be obtained using histogram plots. A random $A_\kappa$ matrix was created for each chain realization and the complete set of odd-numbered eigenvalues was determined numerically and binned to create a normalized set of histograms. The number of independent realizations was 1000 for all cases. We used various widths Δκ for the distributions (where the case is).

The eigenvalue spectrum for the uniform κ distribution shows that the frequencies λ are distributed around the standard chain (Δκ=0) values and the peaks broaden as Δκ increases; the larger Δκ, the larger the width of each peak (Fig. 4.3). There is a high density of eigenvalues at the high λ end. The peaks gradually broaden and completely overlap at high randomness. The lowest eigenvalue $\lambda_{min}$ decreases when Δκ increases.

The histograms for the dichotomous chain (Fig. 4.4) display a different behavior. For small values of Δκ, the spreading about the standard values is still present although the peaks do not display the previously observed symmetry. For larger values of Δκ (0.9), isolated high peaks appear with a quasi-compact domain only at the low end of the spectrum. The peaks become sharper as Δκ increases and arrange in quite symmetrical pattern. Here, the isolated peaks represent the Rouse frequencies of homogeneous chain sections and accordingly, have exact positions. The first peak (small values of λ) moves towards zero as Δκ increases; also its width first broadens with Δκ, but then gets narrower for extreme randomness (Δκ=0.999).

The anomalous chain displays a spectrum with a long tail towards the high frequency limit (Fig. 4.5). The long tail clearly comes from the fact that the anomalous distribution allows for very stiff springs with very short relaxation times. The lowest λ

values form quite a sharp peak which is well isolated from the rest of the spectrum (a $\Delta\lambda \sim 0.1$ gap exists between the first and the second peaks). The lowest eigenvalue, $\lambda_{min}$, is quite large ($\sim 10^{-2}$).

For the exponential distribution, the distribution of eigenvalues resembles the $p_e(\kappa)$ distribution itself. The probability to get very small eigenvalues is large compared with the rest of the spectrum. The smallest eigenvalue, $\lambda_{min}$, is approximately one order of magnitude below the $\lambda_{min}$ obtained for uniform chains and two orders of magnitude smaller than the value observed for the anomalous.

Because the small $\lambda$ limit governs the long time scale relaxation and given the differences we have discussed above, we expect various relaxation responses for the different types of chains we used.

A non-exponential relaxation at long times requires a continuous spectrum near $\lambda=0$. A gap between 0 and the minimum value $\lambda_{min}$ of the spectrum will lead to a single exponential relaxation function after a time t, long enough for the quantity $\exp[-(\lambda_2-\lambda_{min})t]$ to be negligible, where $\lambda_2$ is the next eigenvalue in the spectrum (histogram). The smaller the difference $\lambda_2-\lambda_1$, the larger the time required to observe a single exponential. All the spectra show a nonzero $\lambda_{min}$ although of different magnitudes. Therefore all chains will relax in a simple exponential way after a certain time. The density of the spectra will certainly affect the form of the relaxation and, in the framework of the heterogeneous scenario, we expect better stretched exponential fits for more compact domains.

Before we study the relaxation pattern through the autocorrelation function of the end-to-end vector, it would be interesting to first examine in more detail the relative spacing of the modes for all chain types.

We analyse the relative spacing between the modes for one random realization of each type of chain as well as for many random realizations.

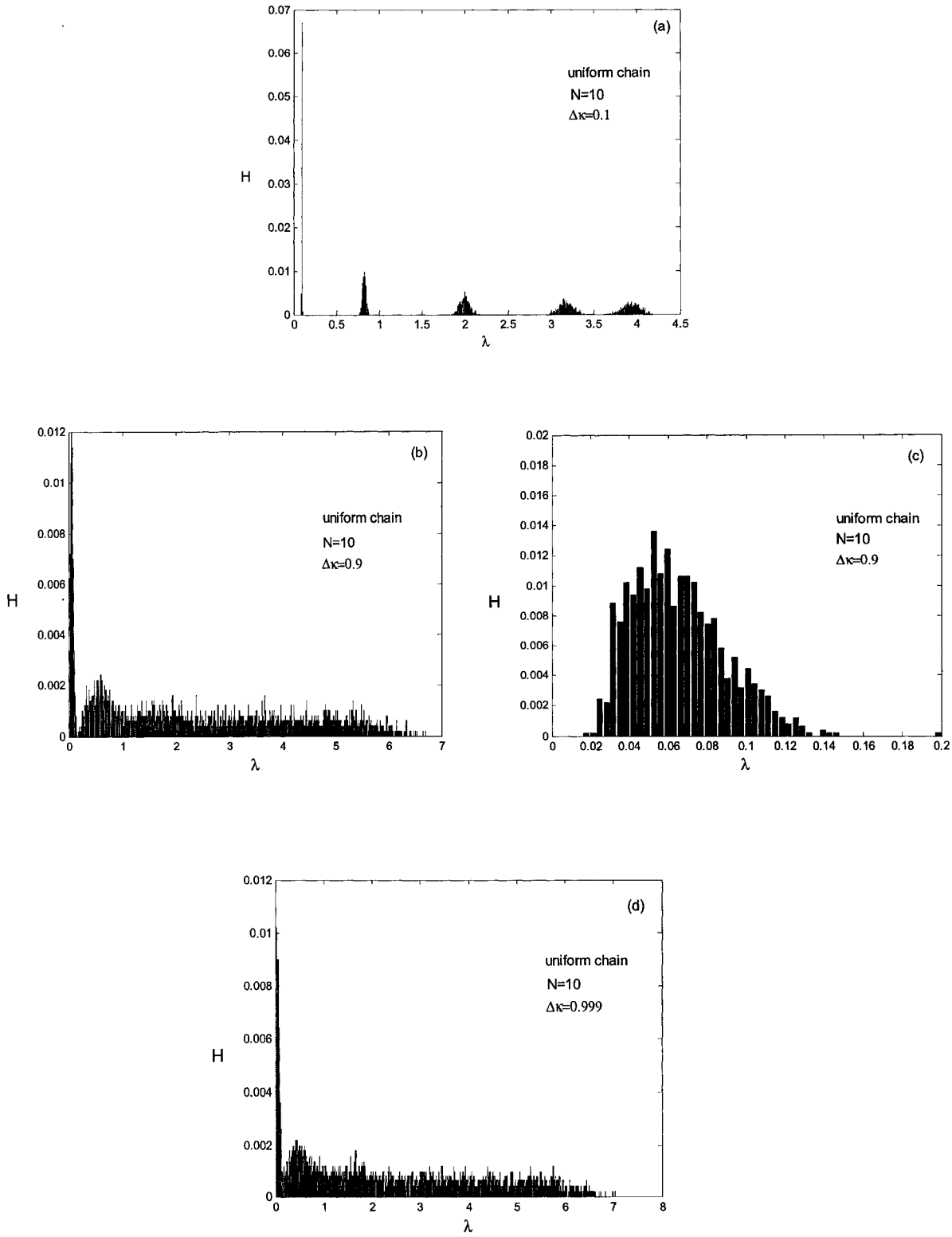


Fig.4.3 Histogram reprezentation of the eigenvalue distributions for random chains that are characterized by the uniform distribution of spring constants. The values of $\Delta\kappa$ are shown. A magnified low end spectrum is shown is one case.

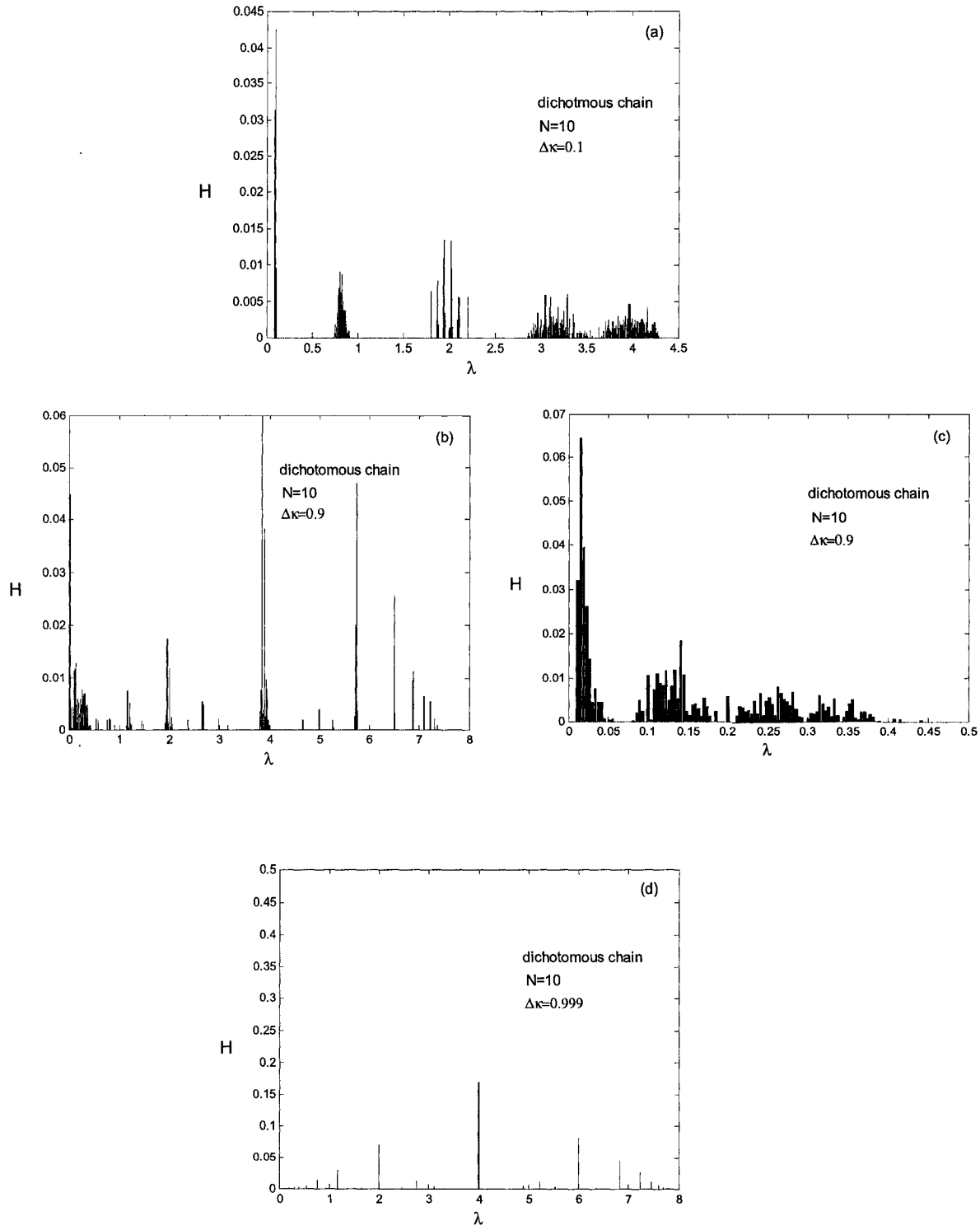


Fig. 4.4 Histograms for the dichotomous chain.

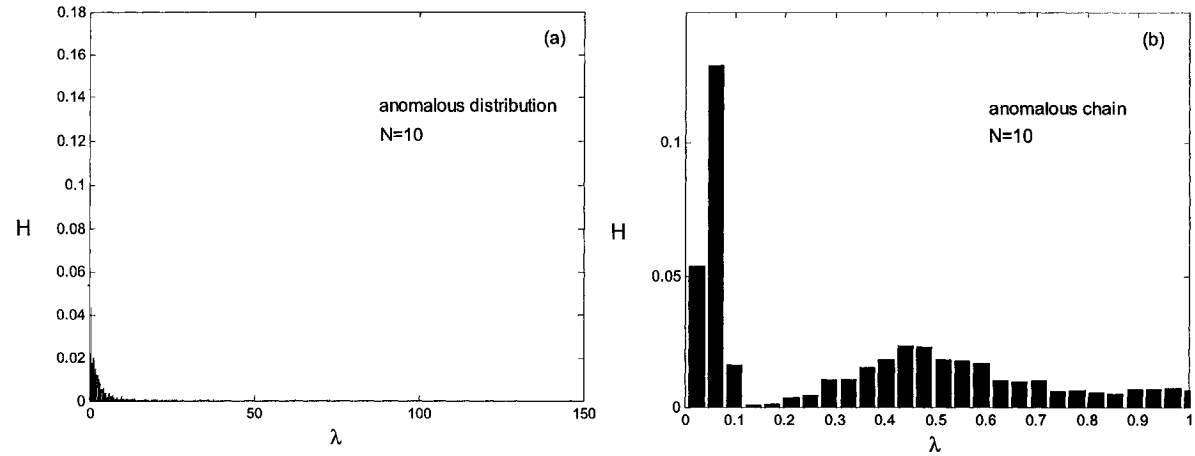


Fig. 4.5 Histograms of the anomalous chain.

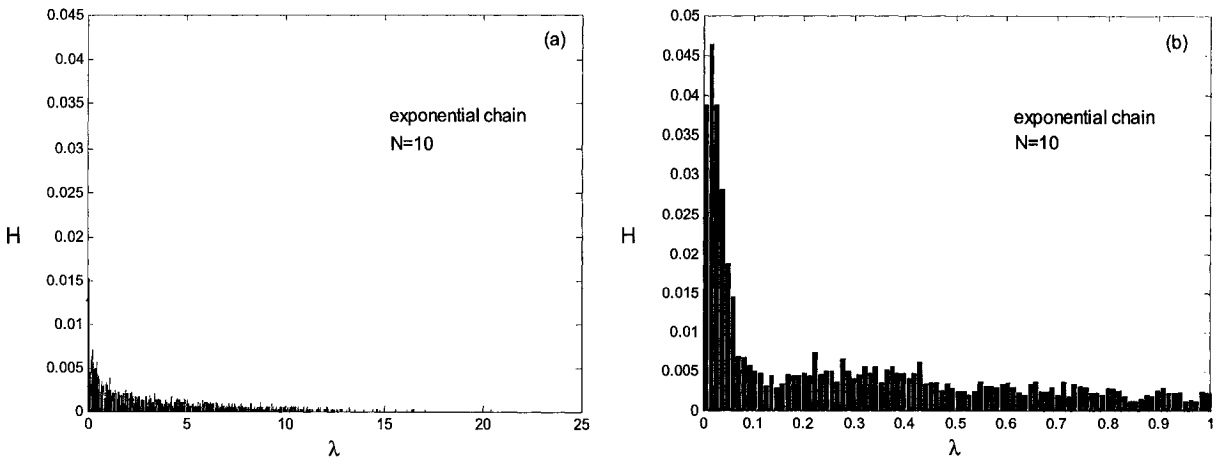


Fig. 4.6 Histograms of the exponential chain.

## 4.4 The spacing between adjacent modes

We have numerically calculated the ratio $r_i$ of the consecutive eigenvalues for a single chain and we plotted it against the eigenvalue index i:

$$r_i \equiv \frac{\lambda_i}{\lambda_{i+1}}. \tag{4.14}$$

Fig. 4.5 shows some examples of $r_I$ values along with the theoretical values for a standard

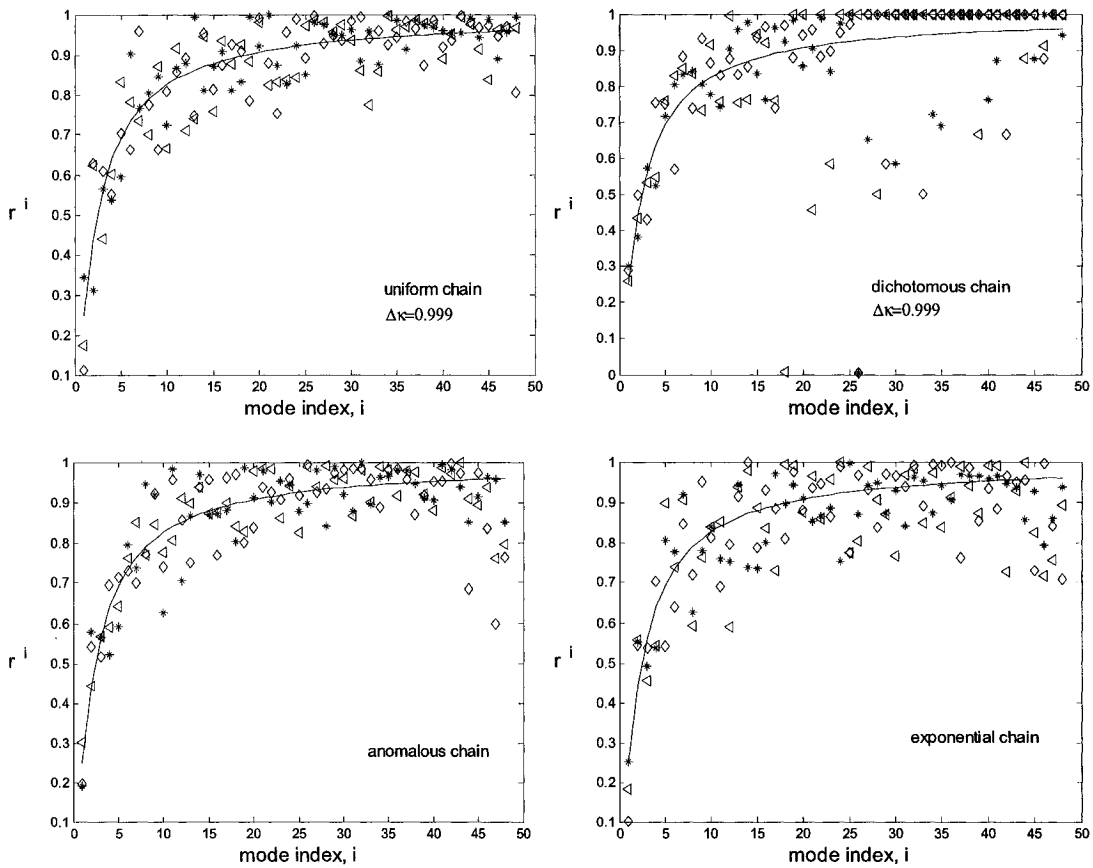


Fig. 4.7 The ratio of the adjacent frequencies against the mode index i, for several N=50 bead chains. The solid line is the prediction for a standard Rouse chain of the same size. The different symbols represent different random chains.

Rouse chain. The relative spacing of the modes typically follows the curve predicted for the classic homogeneus chain. We have obtained similar patterns for many realisations,

and on the average the eigenvalues follow the solid line rather well. They are closer to Rouse curve for small i values, those that are responsible for the long time relaxation.

## *The low frequency ratio*

The overall spacing of the frequencies can be viewed using histogram distributions of a given ratio for many realizations. Because the low frequency modes are dominating in the long time scale relaxation, we only study the ratio between the third and the first mode, $r=\lambda_3/\lambda_1$. We chose these odd mode indices because they are the only ones affecting the end-to-end distance autocorrelation function (see Eq. 2.37 in Chapter 2). Note that $\lambda_3/\lambda_1 \cong 9$ for a long homogenous chain ($\Delta\kappa=0$).

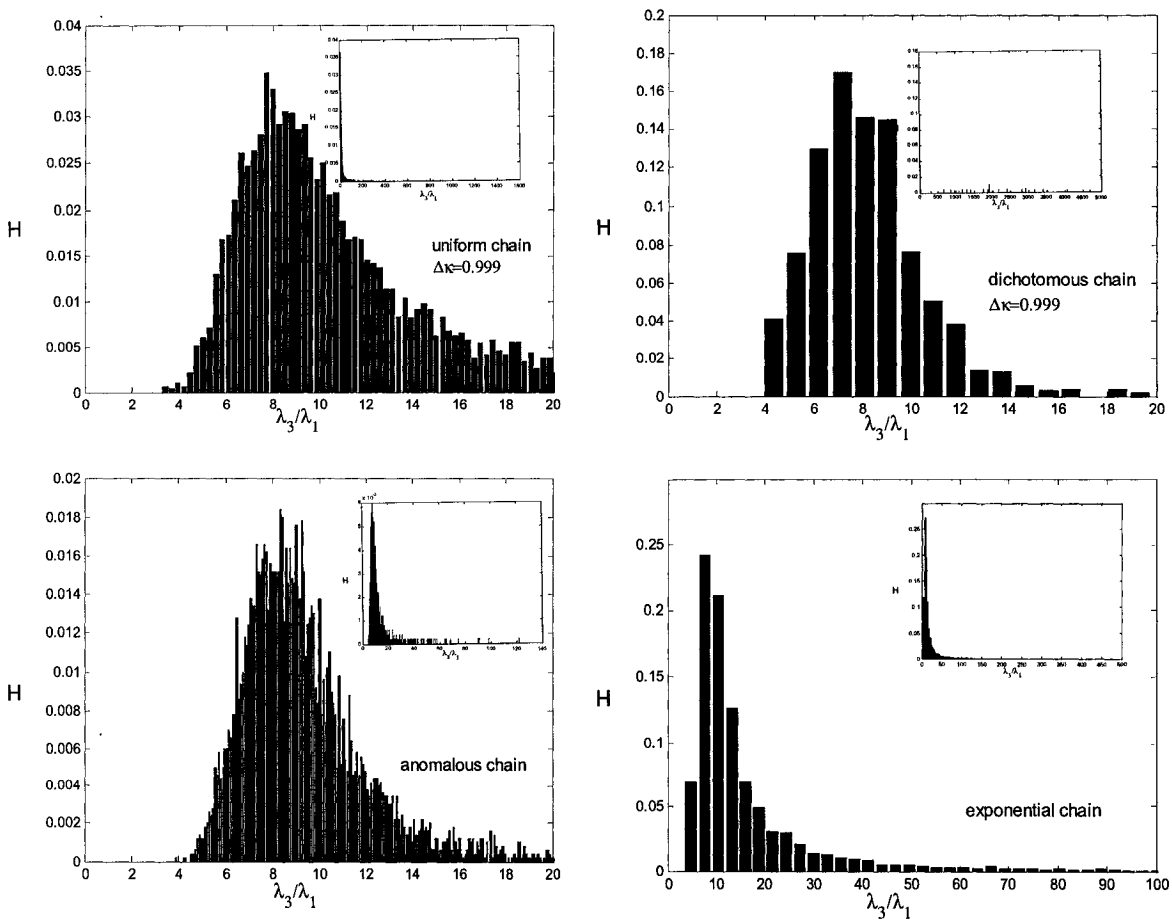


Fig. 4.8 The distribution of ratios $\lambda_3/\lambda_1$ for 5000 realisations of the four types of chains.

All the distribution display an asymmetry around the value 9, the Rouse ratio (see insets). The exponential high limit is even larger then shown. However, these two modes remain well separated in all cases ($\lambda_3/\lambda_1$ never approaches 1). In fact, this can be inferred from the error propagation technique (Ref. 39), by expanding the ratio about its value for the Rouse chain ($\Delta\kappa=0$). To first order, the expectation value of $r_{31}= \lambda_3/\lambda_1$ is well approximated by its value when all the elastic constants are equal. In the same limit, the variance $\sigma_{r31}$ is directly proportional to the variance of the $\kappa$ distributions, i.e.

$$E[r_{31}(\{k_i\})] \approx r_{31}(k) = \frac{\sin^2(3\pi/2N)}{\sin^2(\pi/2N)} \cong 9 - \frac{6\pi^2}{N^2} + O\left(\frac{1}{N^4}\right) \tag{4.15}$$

$$\sigma_{r_{31}}^2 \approx \sum_{i=1}^{N-1}\left[\frac{\partial r_{31}}{\partial k_i}\right]_{k_i=k}^2 \sigma_{k_i}^2 = \sigma_k^2 \sum_{i=1}^{N-1}\left[\frac{\partial r_{31}}{\partial k_i}\right]_{k_i=k}^2 \tag{4.16}$$

We can conclude that on average, the relative spacing of the eigenvalues of a random chain doesn't differ appreciable from the uniform chain case. From the above results we expect negligible differences in the relaxation dynamics of a single random chain relative to the classic Rouse chain. The randomness generates a wide variety of chains, but each of them is behaving essentially like a normal Rouse chain at long times.

## 4.5 The dynamics of a single random chain

The rotational relaxation of a Rouse chain is characterised by the end-to-end distance autocorrelation function C(t). The relevant formula (for a homogeneous chain) was derived in the second chapter (Eq. 2.35) and it is written (normalized so that C(0)=1),

$$C(t) = \frac{\sum_{p:odd integer} \frac{1}{\lambda_p} \exp\left[-\frac{k\lambda_p}{\zeta} t\right]}{\sum_{p:odd integer} \frac{1}{\lambda_p}} . \tag{4.17}$$

Using this expression for the correlation function of a random chain is not exactly correct since the summation is not only over the odd modes anymore. The lack of symmetry

implies that the even modes also contribute. However, the weight of the odd modes are larger than that of the even ones; moreover, they change their sign randomly so that on average their contribution tends to be small. Consequently, the main contribution to the end-to-end distance random chain correlation function still comes from the odd modes and we chose to use the same expression for simplicity. In term of time scales, the error would actually occur for times shorter than $\tau_1/4$, i.e. for short times, and this is not relevant for this study.

In the case of a random chain, the eigenvalues $\lambda_p$ are functions of the random variables $\{\kappa_i\}$, therefore themselves random variables. In our numerical studies C(t) is normalized and the time is scaled as $k_{av}t/\zeta \rightarrow t$.

A simple way to check for a KWW function is the double logarithmic plot that gives a straight line with a subunitary slope equal to the stretched exponent β.

$$\log[-\ln[\exp(-(t/\tau)^{\beta})]] = \beta \log t - \beta \log \tau \qquad (4.18)$$

In order to compare the relative spectra we rescaled t one more time, but differently for each chain, as $t/\tau_1$ ($\tau_1$ is the largest relaxation time for each chain). For small sizes (N=10), the random chains show a clear single exponential relaxation (β=1), starting

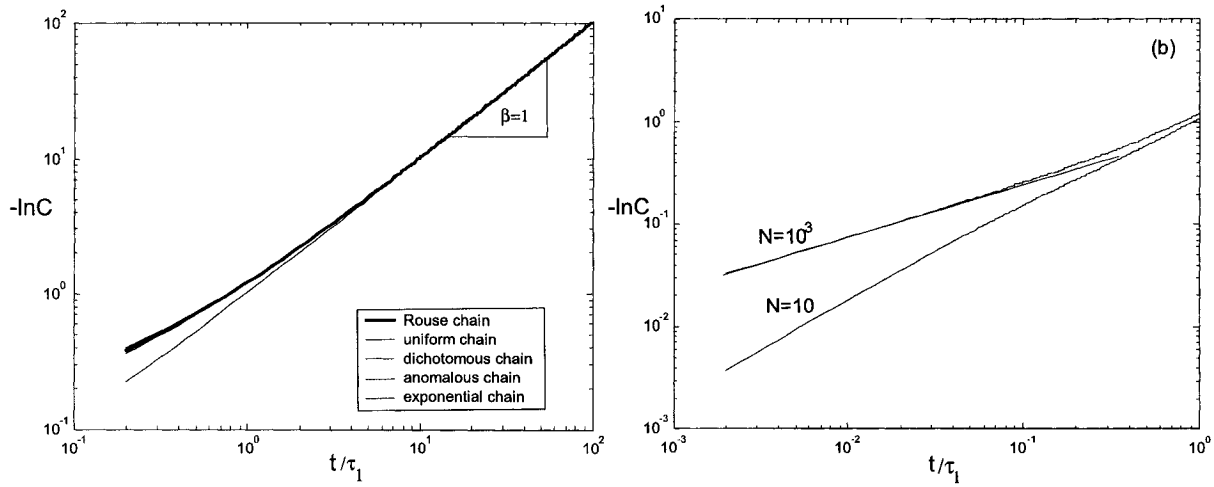


Fig. 4.9 Plot of –lnC(t) versus t in a double logarithmic presentation: (a)-all types of short random chains together with the Rouse chain of the same size (N=10), (b)- dichotomous chains with two different sizes.

with intermediate times ($t/\tau_1 \sim 1$). At very short times, however we cannot distinguish any clear straight line that would cover at least one decade time. For very long chains, the curves tend to be straight lines with subunitary slopes in the short time domain, $t/\tau_1 < 1$ (Fig.4.9.b). The one chain eigenvalue spectrum becomes denser in the high mode domain ($\lambda_{i+1}/\lambda_i \sim (i+1)^2/i^2 \sim 1$) when N increases. This suggests that at least in principle, a possible stretched exponential relaxation exists for very long chains, for times $t < \tau_1$. Moreover, this occurs irrespective of the heterogeneity of the elastic constants, as we can easily see from the figure. The randomness (at least of the types we have considered) becomes less and less relevant as $N \to \infty$.

We can conclude that the randomness (of the types we chose) of a single chain does not affect its long time relaxation, this being practically a standard Rousean relaxation. In the following we study the influence of the same type of randomness upon an ensemble of linear polymers, a case that is actually more closely related to practical measurements.

## 4.6 The relaxation of an ensemble of non-interacting random linear polymers

Let us consider now a system of P random polymers in a dilute solution, that is, without interchain interactions and also in the Rouse limit, i.e. without hydrodynamic or excluded volume interactions. Each chain in the ensemble will independently possess a random structure, according to one of the probability distributions chosen for the elastic constants. In this way we have either a uniform ensemble, a dichotomous ensemble, an exponential ensemble or an anomalous one. The relaxation of such chain ensembles is given by the normalized average over the individual chain relaxations:

$$\langle C(t) \rangle = \frac{\frac{1}{P}\sum_{p=1}^{P}\sum_{i:odd}\frac{1}{\lambda_i(\kappa)\cdot k_{av}}\exp\left[-\lambda_i(\kappa)\frac{k_{av}t}{\zeta}\right]}{\frac{1}{P}\sum_{p=1}^{P}\sum_{i:odd}\frac{1}{\lambda_i(\kappa)\cdot k_{av}}} \tag{4.18}$$

For a large ensemble size, the summation over P transforms into an integral

$$\langle C(t)\rangle \propto \sum_{i:odd} \int_{\lambda_{min}}^{\lambda_{max}} \frac{1}{\lambda_i k_{av}} p(\lambda_i) \exp\left[-\lambda_i \frac{k_{av} t}{\zeta}\right] d\lambda_i \qquad (4.19)$$

for each frequency, where $p(\lambda_i)$ is the probability distribution for mode i. According to the most widely accepted hypothesis, a non-exponential behavior, namely a KWW decay, could be explained by the presence of a broad distribution of $\lambda_i$. This would satisfy the "heterogeneous" scenario.

In the following we show that stretched exponential relaxation appears in these random systems to different extents depending on the type of randomness. We also discuss some relevant features of the KWW regime, analyze the differences among the types of randomness we chose, and propose some explanations for the behavior we observe.

### *4.6.1 An example using the exponential ensemble*

In Fig. 4.10, we examine a typical example (with the exponential distribution function) using a double logarithmic plot. The sizes of the ensemble and of the chain are indicated in the figure. Note that the time axis is rescaled using the average relaxation time $\langle \tau_1 \rangle$ of the P chains of the ensemble. One observes two distinct regimes: a stretched

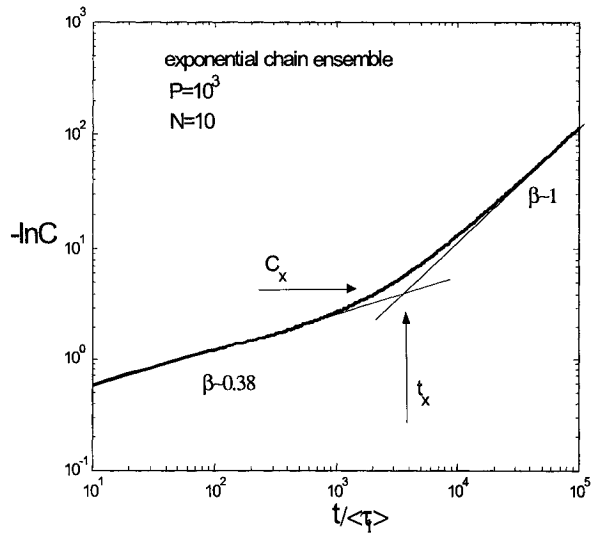


Fig. 4.10 Double logarithmic plot of the correlation function for the exponential ensemble. The crossover point is found at $t_x \sim 3x10^3$ and $C_x \sim 1/e^4$. The relaxation times characterizing the two regimes are $\tau_\beta \sim 150$ and $\tau_\beta \sim 400$.

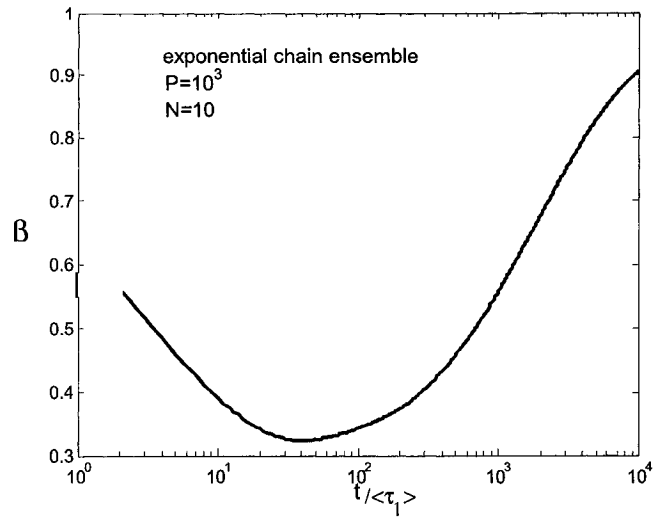


Fig. 4.11 The local β exponent of the previous curve versus time.

exponential domain (with an apparent stretched exponent β~0.38) that gradually goes into a simple exponential decay (β~1) for times longer than ~$10^4$. The intersection point of the two slopes can characterize the crossover regime through both the crossover time $t_x$ and the corresponding correlation amplitude $C_x$. It is important to note that the time interval where the KWW regime appears covers experimentally relevant values, up to $10^3$ times the average relaxation time $<\tau_1>$ of the individual chains. Moreover, the correlation function drops to about $C(t)\sim10^{-2}$ over that time scale. Consequently, a typical experimental measurement would certainly show a clear KWW relaxation for a large time interval.

A detailed view of the relaxation process can also be obtained if we compute the local slope, β, and plot it against time. Figure 4.11 shows that the β exponent actually varies with time. It starts from one, at the beginning of relaxation (not shown in the figure), then monotonically decreases to a minimum, and finally increases asymptotically towards 1 again. In the interval $t/<\tau_1>=10^0-10^3$ the values of β exponent vary between 0.35 and 0.55. These slow variations are practically imperceptible in conventional relaxation measurements. Indeed, we obtain a good fit of the correlation function C(t) with a KWW function on the time interval that would make sense from a practical point of view (Fig. 4.12).

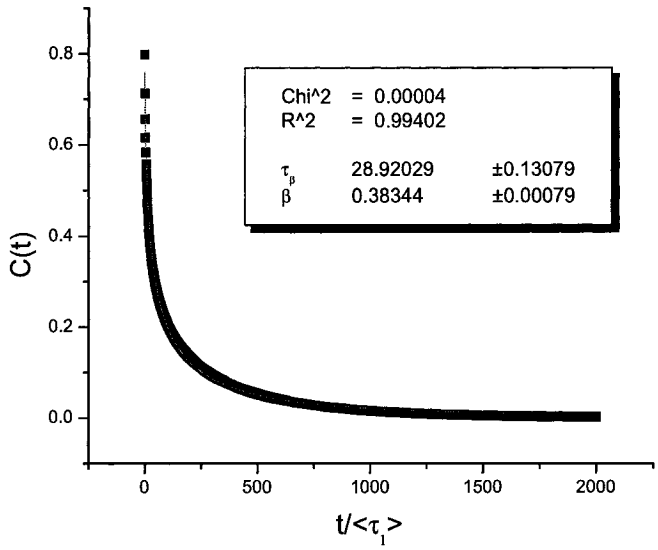


Fig. 4.12 A stretched exponential fit for the exponential chain ensemble in Fig. 4.10. The errors quoted are related to the fitting procedure used by Origin.

While the β coefficient describes the form of the relaxation function, the parameter $\tau_\beta$ provides a generic relaxation time. These will be good criteria to compare different types of chain relaxation. It is interesting to note that for the example presented here, $t_x$ is about 100 times larger than the relaxation time $\tau_\beta$.

### *4.6.2 A look at the four distributions*

In this section we analyze the relaxation of all four random chain ensembles. A double logarithmic representation (Fig. 4.13) shows clear differences among the ensembles. For the uniform and dichotomous ensembles we use the largest possible variance $\sigma_\kappa$. Fist, we notice that the randomness slows down the relaxation (see the results for the standard Rouse chains on the figure) but to different extents: the slowest relaxation is found for the exponential chain system and the fastest one occurs with the dichotomous ensemble but this case is quite close to the clasic Rouse chain. The uniform and the dichotomous chain ensembles display clear KWW-like regimes, over sufficiently

large time periods. In all cases the long time behaviour clearly converges towards a single exponential (β=1).

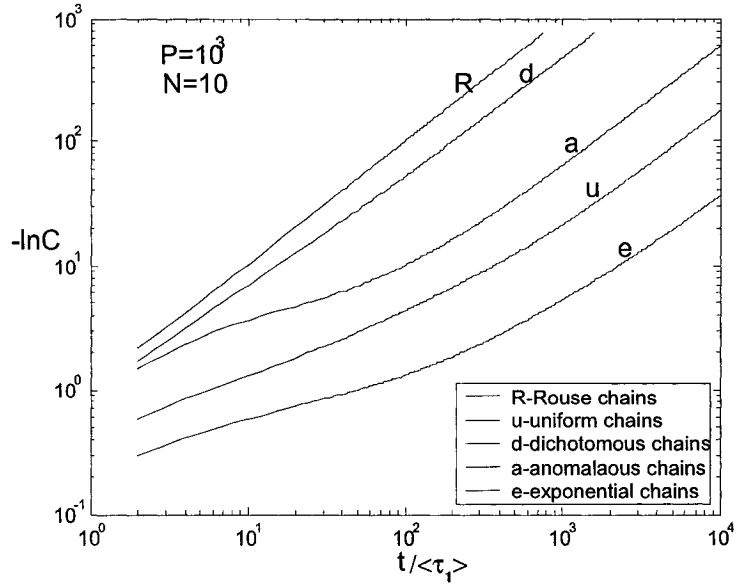


Fig. 4.13. Double logarithmic plot of C(t) for the four ensembles. The R curve has a slope of 1 over the whole time interval shown here.

In Fig. 4.14 we have numerically calculated the KWW parameters, β exponent and the characteristic relaxation time $\tau_\beta$ for the other three ensembles. The β values are the smallest for the exponential ensemble (~0.38) and the largest for the dichotomous one (~0.84). The quality of these fits also varies from one ensemble to the other. The anomalous ensemble doesn't display a clear KWW relaxation.

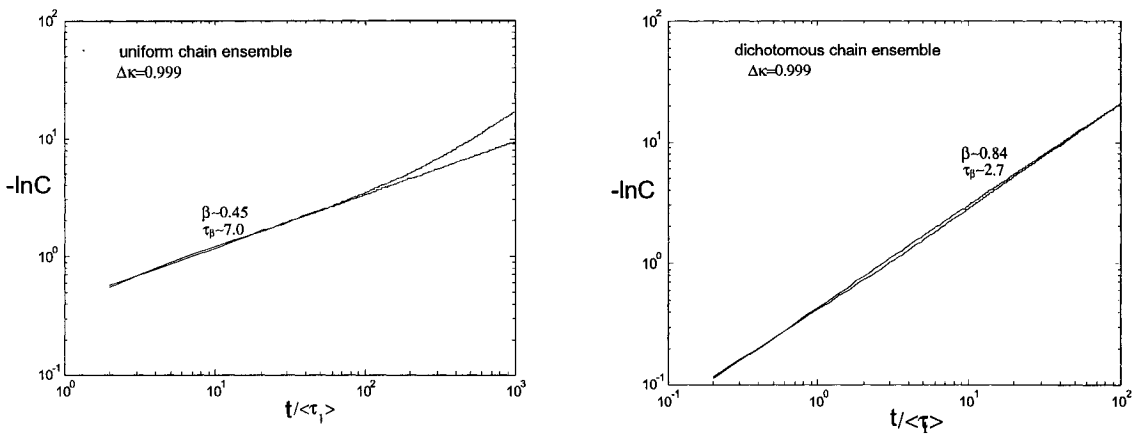


Fig. 4.14 Double logarithmic plots of C(t) for the uniform, dichotomous and anomalous chain ensembles. The chain sizes are N=10 beads and the ensemble sizes are P=500.

These differences in the relaxation behaviour must be directly related to the differences in the eigenvalue spectra. The first observation is the difference in the maximum values allowed for the standard deviation $\sigma_\kappa$ of each distribution. While $\sigma_\kappa$ is fixed to 1 and $\infty$, respectively, for the exponential and anomalous cases, we note that $0 \leq \sigma_\kappa \leq 0.26$ for the uniform and $0 \leq \sigma_\kappa \leq 1$ for the dichotomous distribution. Secondly, the form of the $p(\lambda)$ distribution certainly plays an important role for the occurrence of the KWW decay. There is not any well-established particular form of the distribution $p(\lambda)$ that would lead to a KWW function. According to the heterogeneous scenario (see Eq. 3.1) there are many functions $p(\lambda)$ that potentially can lead to a stretched exponential form of C(t) using the same approximate method of integration. We expect that some $p(\lambda)$ functions favour the occurrence of KWW domain.

Figures 4.15 and 4.16 show that stretched exponentials do provide good fits over relatively long time domains for the uniform and the dichotomous chain ensembles. The dichotomous ensemble KWW interval is the largest one, from very early times up to the time values where $C(t) \sim 10^{-30}$.

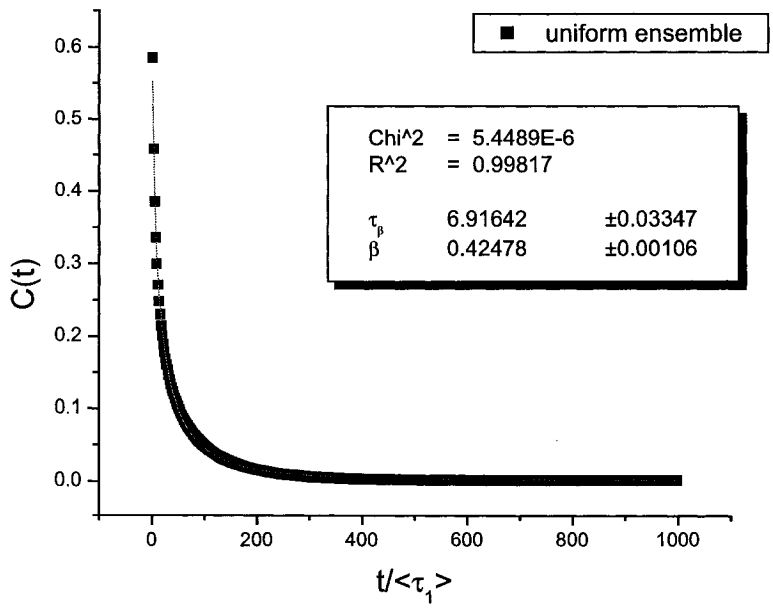


Fig. 4.15 The KWW fit of the correlation function C(t) for the uniform chain ensemble.

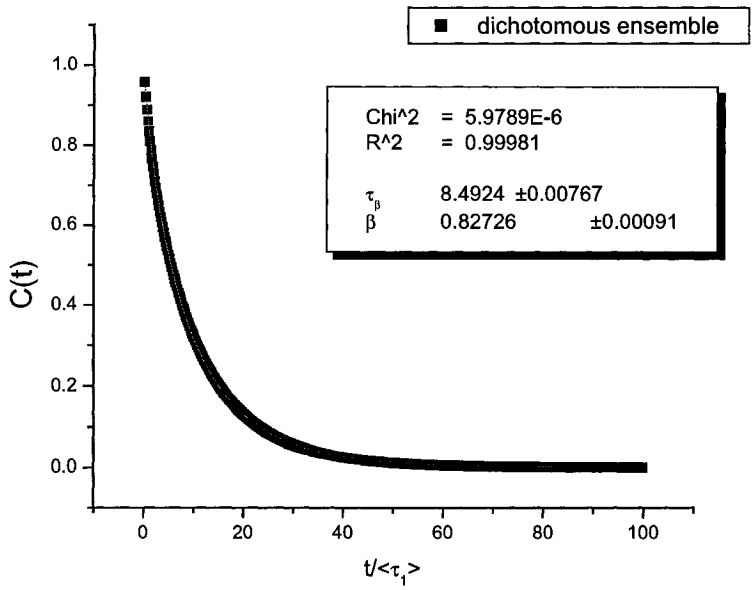


Fig. 4.16 The KWW fit of the correlation function C(t) for thedichotomous chain ensemble.

In these two cases the standard deviation of the κ distributions can vary. We found that the stretched exponent β decreases with increasing disorder (see Fig. 4.17). Consequently, the β exponent can be used as a heterogeneity parameter.

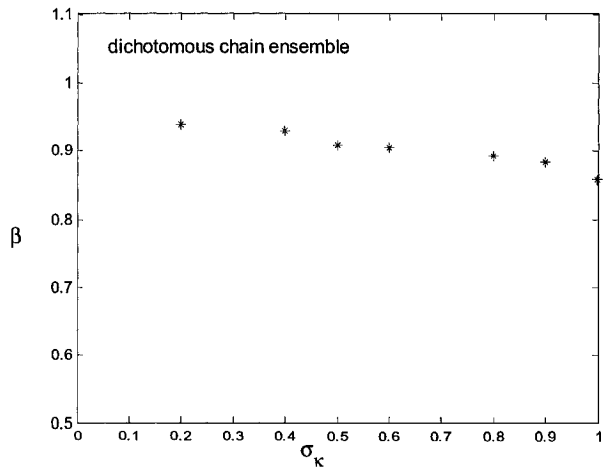


Fig. 4.17 The β coefficient versus the standard deviation $\sigma_\kappa$, for the dichotomous ensemble.

In the following section we study the properties of the β exponent.

### *4.6.3 The universal nature of β for N>>1*

We now examine the molecular-size dependence of the β exponent. In Fig. 4.18a we see a plot of three C(t) functions obtained for different sizes N (also in double logarithmic scale) against the unscaled time t . The crossover time $t_x$ increases with N but the slope of the curves in the KWW domain is approximately constant. The corresponding values for the crossover correlation amplitude $C_x$ remain practically the same. As a consequence, rescaling the time leads to the same curve, as can easily be seen in Fig. 4.18b (here the curves practically overlap). Therefore, the crossover time $t_x$ scales as $N^2$, exactly like the average relaxation time $<\tau_1>$. The chains relax practically in the same manner even if they have different sizes. It is only the type of the randomness that affects the shape of the relaxation function. In other words, β is an intrinsic parameter of disorder.

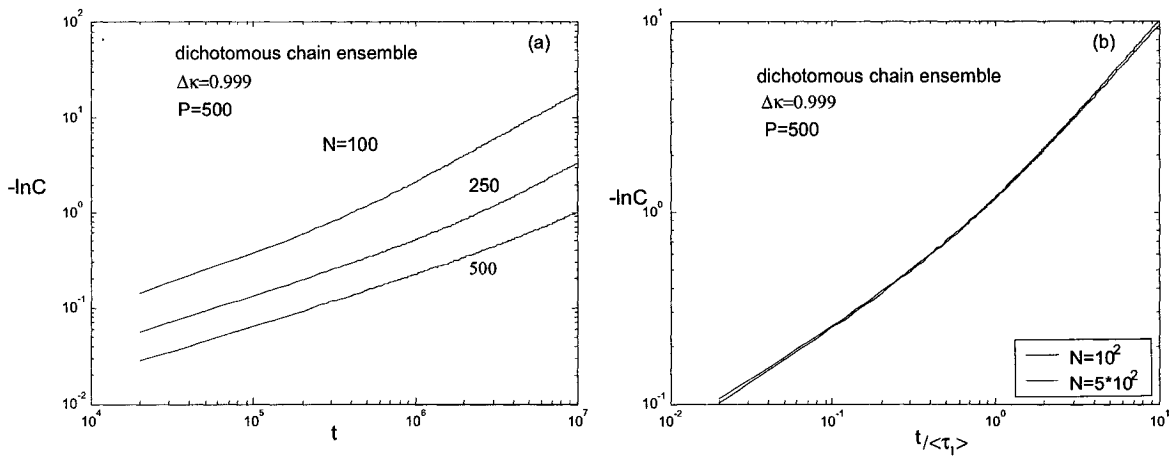


Fig. 4.18 The decay functions for three chains having different sizes. (a) – plotted versus time t and (b) – plotted versus the scaled time, $t/\langle\tau_1\rangle$.

### 4.6.4 *The ensemble size dependence of the KWW regime*

We have shown that stretched exponential relaxation can occur only for ensembles of random chains. In this section we study the influence of the ensemble size on the KWW regime.

According to Eq. 4.19, one necessary condition for the KWW regime to appear is a continuous and broad spectrum of eigenvalues $\lambda_p$. The origin of the stretched exponential decay, a superposition of many exponential processes, suggest that we could recover simple exponential decays both at extremely short and long times. Here, the relaxation rates will be only due to the edge values $\lambda_{min}$ and $\lambda_{max}$ of the eigenvalue

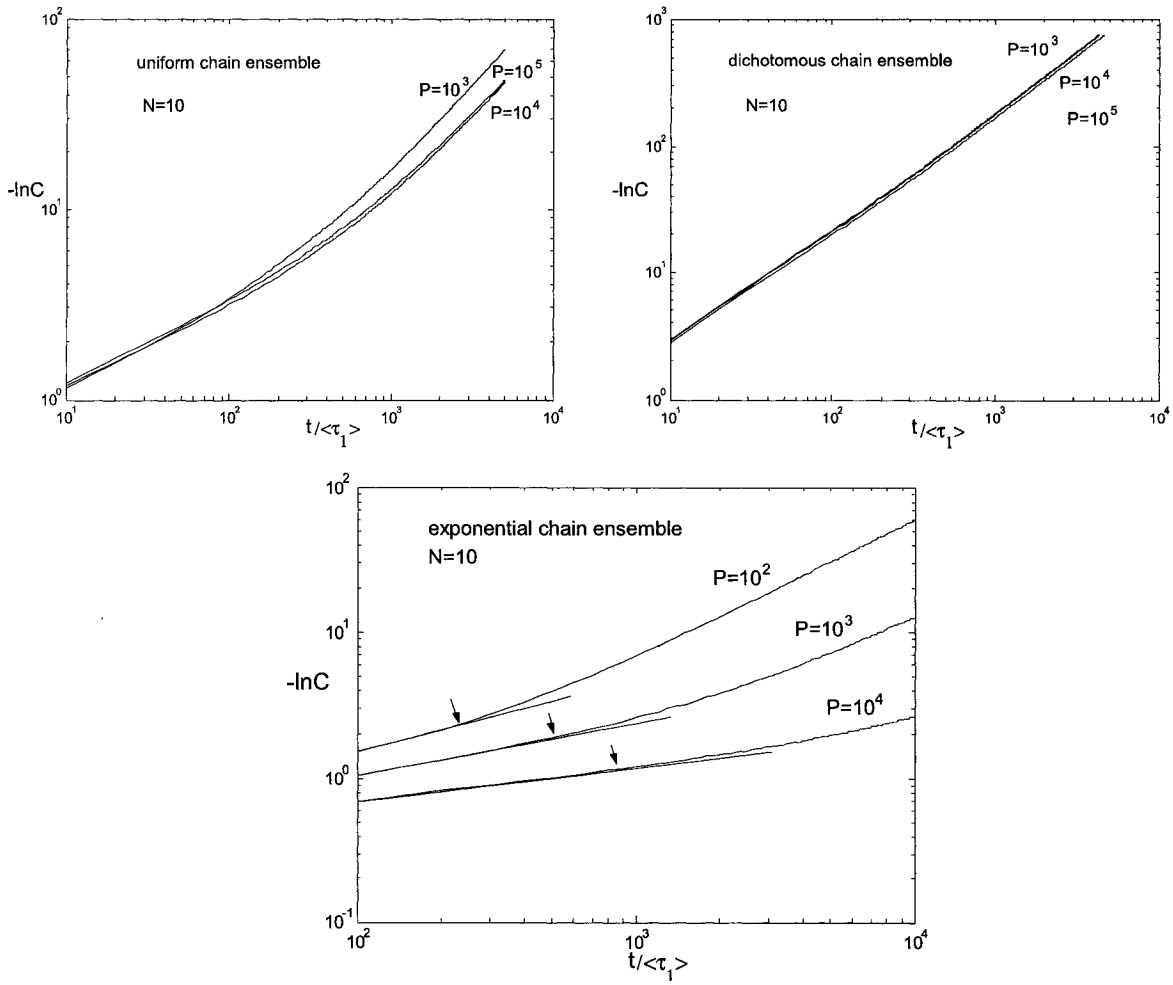


Fig. 4.19 Double logarithmic plots showing how the decay function depends on the ensemble size P.

spectrum. When the ensemble size increases we expect a slight variation of the eigenvalue interval [$\lambda_{min}$, $\lambda_{max}$] because this increases the probability of having extreme cases. Since it is only the long time relaxation that is important in practice, we will examine only the $\lambda_{min}$ limit.

In Fig. 4.19 we present the correlation functions, for all types of ensembles and for various values of the ensemble size P. The behaviour of the ensembles seems to be quite different. The exponential system exhibits the strongest P-dependence while poor ensemble size dependence occurs in the uniform and dichotomous ensembles. We see that in general $t_x$ shifts towards larger values when P increases. The crossover behaviour can be more easily quantified by looking at local β-exponent plots (Fig.4.20) obtained from the local

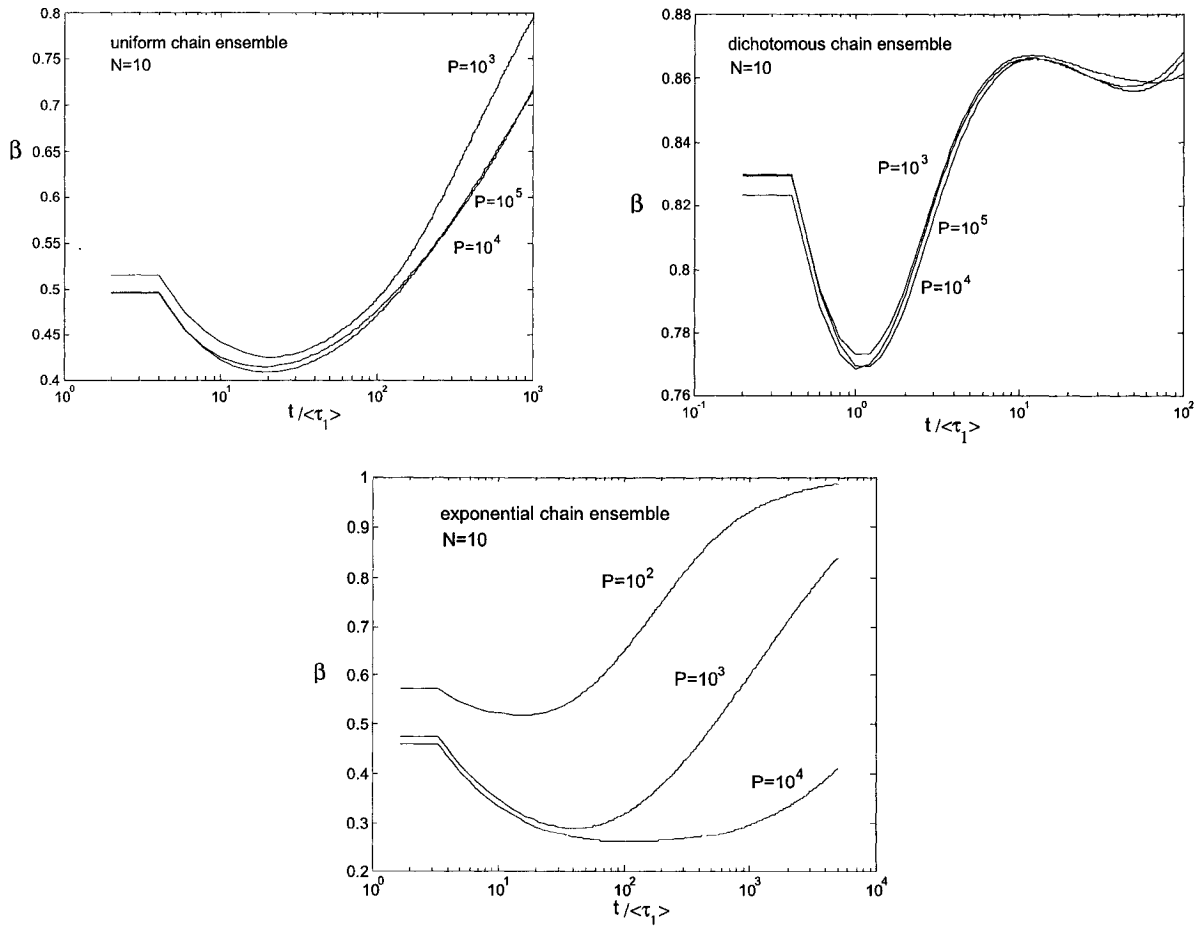


Fig. 4.20 Plot of the local exponent β calculated from the local slope of the corresponding curves in Fig. 4.19.

slopes of the previous curves. Here we identify the crossover time $t_x$ with the minimum of the curves. It was already shown (section 3.4) for other disordered systems (e.g. for spin systems and diffusion in a system with randomly distributed traps, Ref. 34) that the ensemble size dependence is actually an evidence that supports the competing exponential process that occurs during the relaxation. We now apply this derivation to our case and try to give an explanation for the results we obtain.

According to the theory of the competition between two exponential process, KWW type relaxation occurs for the time domain where $n^*$, the value of the integration variable for which the expression under the integral

$$q(t) = \int_0^{n_{max}} p(n)Q(n,t)dn \tag{4.20}$$

is maximum, is much smaller than $n_{max}$. In our case the variable n is associated with the characteristic relaxation times, or equivalently with the normal mode eigenvalues. Namely, we have

$$C(t) = \int_{\lambda_{min}}^{\lambda_{max}} \frac{1}{\lambda} p(\lambda)\exp(-\lambda t)d\lambda \tag{4.21}$$

and the KWW condition becomes $\lambda^*(t) >> \lambda_{min}$ (note that $\lambda_{min}$ plays the role of $n_{max}$ here). The existence of as a narrow peak at $\lambda^*$ requires the following form for the ratio $p(\lambda)/\lambda$

$$p(\lambda) \cong \exp(-\frac{a}{\lambda^\alpha}) \tag{4.22}$$

that is, a sharp descending function when $\lambda \to 0$ (a and $\alpha$ are positive constants). This yields

$$\lambda^* = \left(\frac{\alpha a}{t}\right)^{\frac{1}{1+\alpha}}. \tag{4.23}$$

For very long times, when $\lambda^*(t) << \lambda_{min}$, the relaxation gradually takes the form of a simple exponential with a rate proportional to $\lambda_{min}$. A straightforward test for the competing exponential processes is the crossover time ($t_x$) ensemble size dependence. Following the reasoning in section 3.4, we can assume that $\lambda_{min}$ has the lowest probability and so, if it occurs, it should contain at least one mode. We can accordingly write $\exp(-a/\lambda^\alpha_{min}) \cong 1/P$ which yields

$$\lambda_{\min} \cong \left(\frac{a}{\ln P}\right)^{1/\alpha} . \tag{4.24}$$

From the equality $\lambda^* = \lambda_{\min}$ we then obtain the crossover time

$$t_x \cong \alpha a \left(\frac{\ln P}{a}\right)^{1+1/\alpha} . \tag{4.25}$$

and a weak but measurable logarithmic dependence on P. In Fig. 4.21 we present a plot of $\log(t_x)$ versus the $\log[\ln(P)]$ for the exponential chain ensemble. The linear fit supports the competing exponential process.

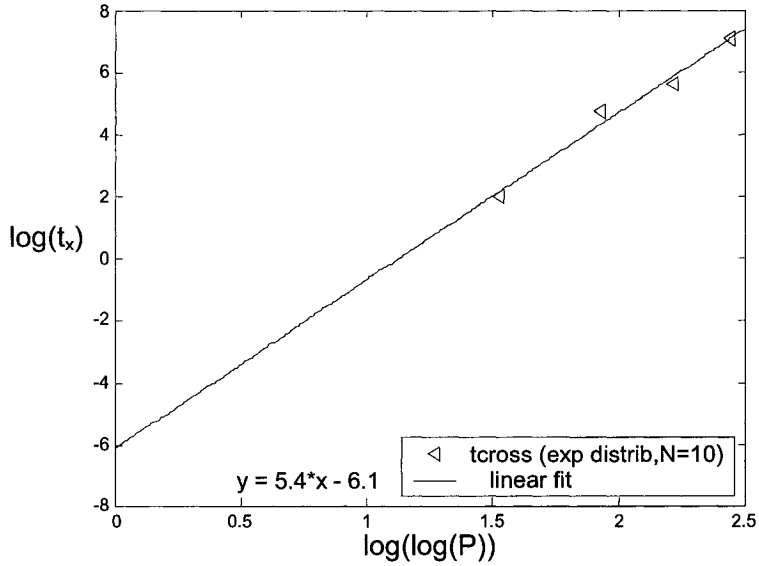


Fig.4.21 The logarithm of the crossover time $t_x$ versus $\log[\ln(P)]$ for the exponential ensemble.

An estimation of the parameters a and $\alpha$ gives roughly $\alpha \cong 1/4$ and $a \cong 3$. The corresponding probability distribution function for the eigenvalues of the exponential system is then

$$p(\lambda) \cong \exp(-\frac{3}{\lambda^{1/4}}) . \tag{4.26}$$

The weak P-dependence in the uniform and dichotomous ensembles seems to be due to the different shape of the $p(\lambda)$ distributions in the $\lambda \to 0$ limit (this influences the long time behaviour). In Fig. 4.22 we plot the $p(\lambda)$ function for three different values of $\alpha$. We see that when $\alpha$ increases the curves drop more abruptly towards zero. Both the dichotomous and the uniform ensembles spectra exhibit sharp descending forms in this

region. Indeed, when we examine Eq. 4.25, we see that large $\alpha$ values lead to a weak P-dependence of the crossover time $t_x$.

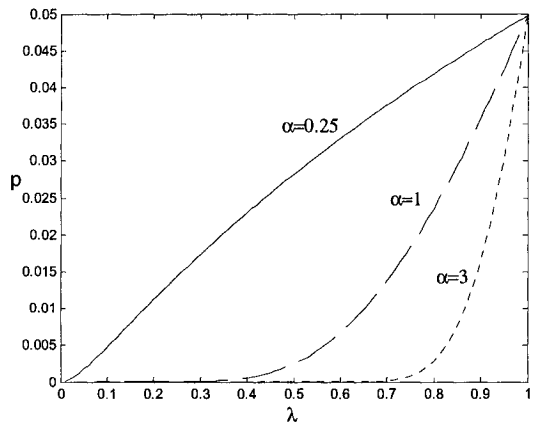


Fig. 4.22 The probability distribution function $p(\lambda) = \exp(-a/\lambda^{\alpha})$ for various values of parameters a and $\alpha$.

## Conclusions

In this chapter, we studied the influence of intrachain disorder on the relaxation of linear polymer chains. We have included the heterogeneity of the elastic spring constant k in the Rouse model for linear polymers. Different types of randomness were considered for k. The probability distributions P(k) we chose for k are the uniform, dichotomous, anomalous and exponential probability. A complete eigenvalue spectrum was calculated numerically while changing the variance of P(k) and the length of the chains. The spectra were analysed in terms of their shape and compactness. The spectra characteristics were further studied through the relative arrangement of the eigenvalues. The consecutive ratio of the modes was calculated for each type of chain and histograms of the lowest eigenvalue ratio were constructed.

We first studied one single random chain relaxation. No significant differences were found between a random chain and the standard Rouse equivalent. This agrees with the fact that, even for a large width of the k probability distributions, the arrangement of the random chain eigenvalues do not appreciable differ from the Rouse counterpart. The consequence of the above is that the relaxation is still exponential starting with early times. However, for very long chains, the presence of numerous eigenvalues at the high

end of the spectrum can lead to a stretched exponential regime at small times. This trivial effect is present even in simple Rouse chains.

However, a clear non-exponential relaxation at long times appears for ensembles of such random polymers. The effect is clearly viewed for systems with only 1000 polymers. Good fits with the KWW function were found for time intervals over which the correlation functions has measurable values for the uniform, dichotomous and exponential cases ($C(t)\sim 1\text{-}10^{-5}$) . At very long times, single exponential relaxation is always recovered. The subunitary exponent $\beta$ appears to be an intrinsic parameter of the system, being sensitive to the width of the $\kappa$ distributions as well as to their form. The finite duration of the KWW regime appears to be a consequence of the finite size of the ensemble. But each type of randomness responds differently to the ensemble size P. For instance, the exponential system is the most sensitive to P. The crossover time $t_x$ shows clear logarithmic dependence on P, which can be considered as a proof for the competing exponential process, the one that is well-known to lead to a stretched exponential relaxation. We believe that the large probability of very small $\kappa$ values, and conversely very small $\lambda$ values, favours this behaviour. On the other hand, the poor P-dependence of the other ensembles could be explained by the particular shape of the spectra in these cases.

The fact that the time interval over which the KWW regime is present increases with the size of the ensemble makes plausible the hypothesis that an infinitely large ensemble of random linear polymers relaxes in a stretched exponential manner for all practical times.

# Chapter 5

## The entropic spring constant of a polymeric chain: stress versus strain ensembles

The aim of this chapter is the study of the elastic behavior of a single linear polymer. More precisely we are concerned with the relationship between the end-to-end distance $\vec{h}$ of the polymer and the force $\vec{f}$ pulling its ends. Various aspects of polymer elasticity are of critical importance in shear flows for technical applications (especially elastomers), in biology, in DNA gel electrophoresis where the force law must be used to represent the tension in the links between electrically charged segments, in DNA replication, for muscle contraction etc. Recently, single molecule experiments have been made possible and we can now make direct measurements of the forces generated in biochemical reactions. In these experiments, the elastic behavior of single DNA molecules and the unfolding of proteins are being investigated. The elastic response of a chain is linear only for small extensions (forces up to about 0.003pN for DNA, (Fig. 5.1).

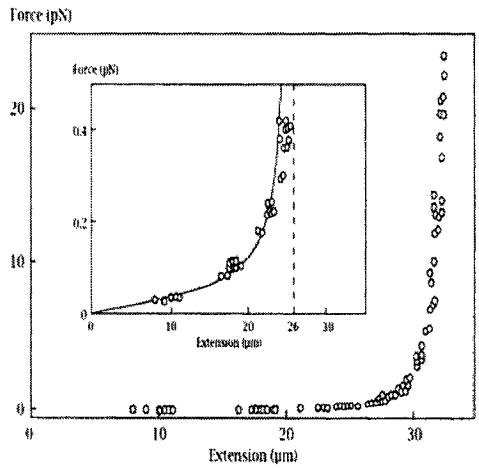


Fig. 5.1 An experimental plot of the pulling force versus the elongation for DNA. The maximum extension of this DNA molecule is 32.7μm (from Ref.30)

Here a Hooke's type law connects the relative extension and the reduced force:

$$fh_0 / k_B T = 3h / h_o , \tag{5.1}$$

where $h_0$ is the end-to-end distance (in the mean square sense) of the polymer in its unperturbed state. The elasticity is purely entropic since the internal energy doesn't change with the deformation. The pulling forces must overcome the decrease in entropy as the chain extends:

$$f = -T\left(\frac{\partial S}{\partial L}\right)_T . \tag{5.2}$$

where L is the generic elongation of the chain. However, the entropic regime (Eq. 5.2) also includes nonlinear forces when the probability distribution function for the end-to-end distance is not Gaussian (Eq. 5.1 actually corresponds to a Gaussian distribution).

The results for single molecule measurements turn out to depend on which variables are held fixed and which are allowed to fluctuate (in this case $\vec{f}$ or $\vec{h}$) because the fluctuations are now important. But in the thermodynamic limit (a single molecule with an infinite number of monomers) one expects similar force-extension relations. When the force is the controlled variable and $\vec{h}$ is allowed to fluctuate we speak of the f-ensemble (or stress ensemble), whereas we call the h-ensemble (or strain ensemble) the system where $\vec{h}$ is fixed and $\vec{f}$ fluctuates.

When a chain is in out of equilibrium conditions, one needs a nonlinear entropic spring potential in order to preserve its finite extensibility (harmonic springs can stretch to infinity under tension). Unfortunately, the exact conformational average $\langle h^2 \rangle = Nb^2$ is not always recovered with such nonlinear potentials. In the f-ensemble, for instance, we obtain chains that are more compact than expected. Since the f-ensemble problem can be solved exactly, it is nevertheless the most commonly used approximation. As we will demonstrate, one should use the h-ensemble to preserve the mean equilibrium size. The mathematical difficulties encountered in the treatment of the h-ensemble make it a rare bird in the physical sciences even though it satisfies the exact relation $\langle h^2 \rangle = Nb^2$. We will show here how one can generate approximate solutions to this problem (in the form of Padé approximants) with any desired degree of accuracy.

In the first section we describe the classic elasticity laws obtained in the two thermodynamic ensembles, and then discuss the results for the FJC (Freely-Jointed Chain) for different size regimes. A more recent result (Ref. 24) for the force-extension relation in the h-ensemble, which allows for a generalized freely jointed chain without being restricted to rigid segments, is then presented in the next section. In the last section, we construct simpler analytical expressions for this result, for the classical rigid-rod FJC, using systematic rational approximations (modified Padé approximants). This method was previously designed for the f-ensemble formalism (Ref. 23), is applied here for the force extension relation in the h-ensemble.

## 5.1 The stress and strain ensembles for a single polymer chain

When a linear molecule is constrained to have the end-to-end distance $\vec{h}$ fixed, the average force required to maintain this constrain is

$$\left\langle \vec{f} \right\rangle_h = \left( \frac{\partial F}{\partial \vec{h}} \right)_T = -k_B T \left( \frac{\partial \ln Z_h}{\partial \vec{h}} \right)_T \tag{5.3a}$$

where the Helmholtz free energy F is related to the partition function $Z_h$ via the standard relation

$$F_H = -k_B T \ln(Z_h) . \tag{5.3b}$$

Thermodynamically, this is equivalent to the isothermal-isochoric or Helmholtz ensemble where $\vec{f}$ and $\vec{h}$ replace the traditional p (pressure) and v (volume) macroscopic variables.

When the force-extension relation is measured in an experiment with $\vec{f}$ fixed, we have

$$\left\langle \vec{h} \right\rangle_f = -\left( \frac{\partial \Phi}{\partial \vec{f}} \right)_T = k_B T \left( \frac{\partial \ln Z_f}{\partial \vec{f}} \right)_T \tag{5.4a}$$

where the partition function for the isothermal-isobaric system (or Gibbs ensemble) $Z_f$ is related to the thermodynamic potential or Gibbs energy, $\Phi$, via the relation

$$\Phi = -k_B T \ln(Z_f) . \tag{5.4b}$$

We now describe in more details the two ensembles.

## h-ensemble

This ensemble is appropriate in the following experiment (Ref. 31). One end of the molecule is attached to a rigid support and the other is attached to a bead held in an optical trap. The separation of the ends is kept fixed by controlling the bead position through adjusting the trap center to cancel the position fluctuations. The fluctuating force required to do this is measured as a function of time. At each location of the trap, the average force can be measured, such that a plot of the mean force $\left\langle \vec{f}(\vec{h}) \right\rangle$ as a function of the end-to-end distance can be obtained. In these conditions, the potential energy of the molecule at a given extension is a free energy $F_H$ (Helmholtz free energy) and it can be written as an integral over the mean force (actually the quasi-static work performed on the molecule)

$$F_H(\vec{h}) = \int_0^h \left\langle \vec{f}(\vec{h}') \right\rangle \cdot d\vec{h}' \tag{5.5}$$

The free energy is related to the probability distribution function $W_0(\vec{f})$ of the end-to-end distance in the absence of the force

$$F_H(\vec{h}) = C(T) - k_B T \ln(W_0(\vec{h})), \tag{5.6}$$

where $W_0$ is the ratio between the function $Z_h$ and the partition function of the free molecule, Z, i.e.$W_0=Z_h/Z$. We see indeed that the above equations lead to Eq. 5.3.

For a molecule modeled by a FJC, an approximate expression for $W_0$ was given by Kuhn and Grun in the limit of large N (Ref.1),

$$W_0 = B \exp\left\{ -\frac{1}{b} \int_0^h \beta dh \right\} \tag{5.7}$$

where

$$\beta = L^{-1}\left( \frac{h}{Nb} \right) \tag{5.8}$$

is the inverse Langevin function, L(x)≡coth(x)-1/x, of the reduced extension h/Nb and B is a constant. The average force is then

$$\langle f \rangle_h = \frac{k_B T}{b} L^{-1}(h/Nb), \qquad N >> 1. \tag{5.9}$$

Finally, for a Gaussian chain, i.e.,

$$W_0(h) = (3/2\pi Nb^2)\exp\left(-\frac{3h^2}{2Nb^2}\right) \tag{5.10}$$

one gets

$$\langle f \rangle_h = k_B T \frac{3h}{Nb^2} = \frac{3k_B T}{\langle h_0^2 \rangle} h, \tag{5.11}$$

namely, Hooke's law. The entropic elastic constant of the chain in the harmonic limit is then,

$$k = \frac{3k_B T}{\langle h_0^2 \rangle}. \tag{5.12}$$

## f-ensemble

This ensemble has to be used in AFM (atomic force microscopy) experiments when a constant force is applied to the ends of a single protein molecule. One end of the molecule is attached to a support and the other has a magnetic bead (Ref. 31). When placed in a magnetic field gradient, the molecule experiences a force that has no fluctuations. But the end-to-end distance $\vec{h}$ fluctuates and its average in the direction of the applied force is:

$$\langle \vec{h} \rangle = \int \vec{h} W_f(\vec{h}) d\vec{h} \tag{5.13}$$

where $W_f$ is the probability distribution function of the end-to-end distance of the chain that is stretched by the external force $\vec{f}$. The probability distribution $W_f$ can be written as

$$W_f(\vec{h}) = \frac{W_0(\vec{h})\exp(\vec{f}\cdot\vec{h}/k_B T)}{\int W_0(\vec{h})\exp(\vec{f}\cdot\vec{h}/k_B T)d\vec{h}} = \frac{Z_h \exp(\vec{f}\cdot\vec{h}/k_B T)}{Z_f}. \tag{5.14}$$

If we use the relation between the two partition functions, namely

$$Z_f = \int Z_h \exp(\vec{f}\cdot\vec{h}/k_B T)d\vec{h} \tag{5.15}$$

we can easily see that the Gibbs relation (Eq. 5.4a) is obtained.

An important observation can be made if we write $\langle \vec{h} \rangle$ as (from Eqs. 5.13 and 5.14)

$$\langle \vec{h} \rangle = Z_f^{-1} \int \vec{h} Z_h(\vec{h}) \exp(\vec{f} \cdot \vec{h} / k_B T) d\vec{h} = Z_f^{-1} \int \vec{h} \exp[(\vec{f} \cdot \vec{h} - F(\vec{h})) / k_B T] d\vec{h} \quad (5.16)$$

If the fluctuations of h are small or, equivalently, if the distribution $W_f$ has a sharp peak at $\vec{h} = \vec{h}^*$ (the most probable value of the extension), then $\langle \vec{h} \rangle = \vec{h}^*$. The value of $\vec{h}^*$ is then a solution of the equation

$$\vec{f} = \frac{\partial F_H(\vec{h})}{\partial \vec{h}} . \quad (5.17)$$

But this is in fact the general force-extension relation for the h-ensemble. In other words, the two ensembles converge in the thermodynamic limit (the molecular size N is very large), i.e. when the fluctuations are negligible.

Returning to the FJC molecule, one obtains the following exact expression for the f-h relation in the f-ensemble (see Ref. 1):

$$\langle h \rangle_f = Nb\, L(fb/k_B T) \quad (5.18)$$

This is the inverse of the approximate Kuhn-Grun force-extension relation in the h-ensemble but, unlike Eq. 5.7, the above equation is valid for any value of N.

When the molecule is a Gaussian chain ($W_0$ is a Gaussian function, see Eq. 5.10) one finds again the simple harmonic law

$$\langle h \rangle_f = \frac{1}{3} \frac{f}{k_B T} Nb^2 = \frac{1}{3} \frac{f}{k_B T} \langle h_0^2 \rangle . \quad (5.19)$$

The Gaussian limit is thus the second situation when the two ensembles give the same results. An interesting observation was made in Ref. 32. If $W_0$ is Gaussian, the Boltzmann probability distribution function $W_f(h) \propto \exp\{(\vec{f} \cdot \vec{h} - ah^2/2)/k_B T\}$ is symmetric about $h^*$ and we obtain $\langle \vec{h} \rangle_f = \vec{h}^*$ regardless of the magnitude of the macroscopic fluctuations. Thus the two experiments (or equivalently the two ensembles) are identical if the free energy is a quadratic polynomial in h.

Not surprisingly, the harmonic case is recovered in the limit of small forces, i.e. when only the first term is considered in the expansion of the Langevin function

$$\langle h \rangle_f = Nb\left\{\frac{1}{3}(fb/k_BT) - \frac{1}{45}(fb/k_BT)^3 + \ldots\right\} \quad . \tag{5.20}$$

In the opposite limit (large forces), the exact f-h relation (Eq. 5.18) can be very well approximated with the following expression (using $L(x) \approx 1 - 1/x$ when $x \to \infty$)

$$\langle h \rangle_f \approx Nb\left(1 - \frac{1}{fb/k_BT}\right) \tag{5.21a}$$

In reduced variables the above expression can be rewritten as

$$F = \frac{1}{1 - \langle H \rangle_f} \quad . \tag{5.21b}$$

where $\langle H \rangle_f = \langle h \rangle / Nb$ is the reduced average end-to-end distance in the force direction and $F = fb/k_BT$ is the reduced force. This does not agree with the Warner empirical approximation (when the extension is large), extensively used in analytical and computational studies

$$F_{Warner} = \frac{3H}{1 - H^2} \underset{H \to 1}{\to} \frac{3}{2(1-H)} \, . \tag{5.22}$$

Warner's approximation correctly recovers the harmonic term (3H) as well as the finite extensibility ($H \leq 1$), but overestimates the force by a factor of 3/2 for large extensions.

## 5.2 The force-extension relation for a generalised freely-jointed chain in the h-ensemble

In this section we study the force-extension relation for a FJC in the h-ensemble. From the mathematical point of view, this requires a rather complicated calculus apparatus, even for the simplest model, the FJC. An exact expression for the probability distribution function $W_0$ of a FJC was calculated by Treloar:

$$W_0\left(\vec{h}\right)=\frac{1}{8\pi b^2 h}\frac{N^{N-2}}{(N-2)!}\sum_{s=0}^{k}(-1)^s\frac{N!}{s!(N-s)!}\left(m-\frac{s}{N}\right)^{N-2} \tag{5.23}$$

where

$$m=\frac{1}{2}\left(1-\frac{h}{Nb}\right).$$

The upper limit of the summation, k, is determined by the condition

$$k\le mN\le k+1$$

where k is an integer. Because of its complicated form, it cannot easily be used in analytical calculations. Instead, it is mainly used as a reference for analytical approximations. The best approximation (to our knowledge) of the Treloar expression has been recently derived by Glatting et al (Ref. 24). These authors are also the first to provide a microscopic interpretation of the FJC segments that allows for internal degrees of freedom inside each segment. Thus the probability distribution (or equivalently the partition function) is refined to include some correlations between the bonds (see the Appendix for a detailed presentation of this work). In the case of the classic FJC, their approximation gives the following result for the $Z_h$ function:

$$Z_h=\left(\frac{constant}{A_{xx}A_{yy}A_{zz}}\right)^{1/2}\exp\left\{-\frac{\beta h}{b}+N\ln\left[\frac{\sinh(\beta)}{\beta}\right]\right\} \tag{5.24a}$$

where

$$A_{xx}=A_{yy}=b^2\left[\coth(\beta)-\frac{1}{\beta}\right]\frac{1}{\beta} \tag{5.24b}$$

$$A_{zz}=b^2\left[\frac{1}{\beta^2}-\frac{1}{\sinh^2\beta}\right]. \tag{5.24c}$$

The average contractile force is:

$$\left\langle\vec{f}\right\rangle_h=\frac{k_BT}{b}\left[\beta+\frac{b}{2}\frac{d}{dh}\ln\left(A_{xx}A_{yy}A_{zz}\right)\right] \tag{5.25}$$

where

$$\beta=L^{-1}\left(\frac{h}{Nb}\right). \tag{5.26}$$

The second term in Eq. 5.25 is negligible when N>>1, and we then find the Kuhn and Grun force extension relation (Eq. 5.9). The latter being also the exact force-extension relation for a FJC in the stress ensemble, one can see that the second term in 5.25 is actually the difference between the two ensembles in the form of a 1/N term, as the general thermodynamics would predict.

Even for small values of N, this force-extension relation gives an excellent approximation of the Treloar exact function, as the picture below shows.

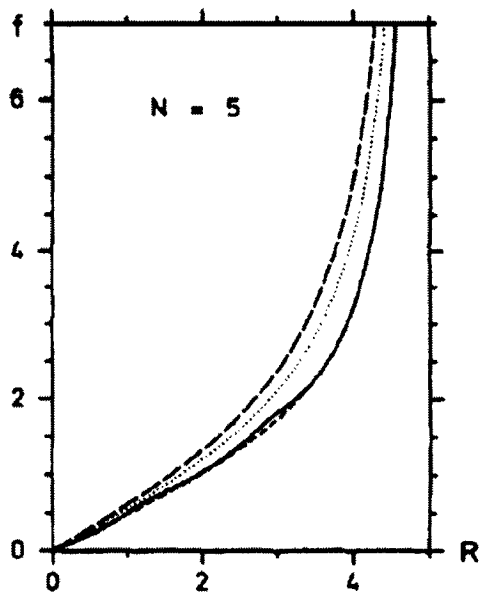


Fig. 5.2 A plot of the force f versus the elongation R taken from the original paper (Ref. 24). Equation 5.24 (---) is the best approximation to the exact formula of Treloar (solid line). The Kuhn and Grun result (---) and an improved formula of Flory (...) are given also.

Unlike Treloar's result, Eq. 5.24 is analytical. However, its complicated form, which includes the derivative of inverse hyperbolic functions, makes it hard to use in practice. In computer simulations, for instance, using such a function would be quite inefficient. We will show in the following that this novel formula can be replaced by a family of very good rational approximations with small errors even for small values of N.

## 5.3 Modified Padé approximants for the contractile force in the strain ensemble

In this paragraph we develop a Padé approximant method for the force extension relation obtained by Glatting et al. (Ref. 24). This method uses ratios of polynomials instead of the original function, with any desired degree of precision.

The two limits of Eq. 5.25 are:

$$\left\langle \vec{F} \right\rangle_H = \begin{cases} (3-3\frac{1}{N})H + (\frac{9}{5} - \frac{99}{25}\frac{1}{N})H^3 + (\frac{297}{175} - \frac{837}{175}\frac{1}{N})H^5 + O(H^7) \equiv F_0, & H << 1 \\ \frac{N-2}{N(1-H)} + \frac{1}{NH} \equiv F_\infty, & 1-H << 0 \end{cases} \tag{5.27}$$

when the following reduced quantities are used:

$$\left\langle \vec{F} \right\rangle_H = \frac{\left\langle \vec{f} \right\rangle_h b}{k_B T} \quad \text{and} \quad H = \frac{h}{Nb} \tag{5.28}$$

The harmonic approximation is found in the small stretching regime, for N→∞, and the asymptotic limit (H close to unity) shows a very good agreement with the Treloar exact formula (when H→1 in Treloar formula, we have k=1 for the limit of the summation and, after simple algebra ones find exactly the same expression for $F_\infty$.). An analytically simple interpolation formula that preserves these limits and has small deviations in the intermediate regime is needed.

Our method first finds a Padé approximation for the series expansion $F_0$, valid in the small stretching limit, followed by consecutive corrections in order to also acquire the necessary asymptotic behaviour, $F_\infty$. We will denote by Padé(H, i, j) the Padé approximant of the $F_0$ series; the numerator Num(H,i) is an i-th order polynomial and Den(H,j), the denominator is a polynomial of order j:

$$Pade(H,i,j) = \frac{Num(H,i)}{Den(H,j)} \tag{5.29}$$

The sum i+j must not exceed the highest exponent of the original (truncated) series expansion $F_0$ in order to assure a complete determinable set of coefficients for the Padé ratio.

The needed divergence in the high streching limit (H=1), can be acquired if one adds an extra term in the form $A \cdot H^k$ to the denominator, such that A=-Den(1,j)

$$\frac{Num(H,i)}{Den(H,i)} \rightarrow \frac{Num(H,i)}{Den(H,j) - Den(1,j) \cdot H^k} \,. \tag{5.30}$$

An exponent k≥j insures that our correction term has a minimal effect on the accuracy of the function, for small values of H. Note that the modified denominator can then be written as g(H)x(1-H), thus correctly reproducing the $F_\infty \sim 1/(1-H)$ divergence found in Eq. 5.27.

Furthermore, the correct asymptotic behaviour $F_\infty$ can be achieved with the addition of a term $B \cdot H^m$ with m≥i, to the numerator, i.e.

$$\frac{Num(H,i) + B \cdot H^m}{Den(H,j) - Den(1,j) \cdot H^k} \quad . \tag{5.31}$$

such that B verifies the following condition:

$$B = \lim_{H \to 1} [(Den(H,j) - Den(1,j) \cdot H^k) F_\infty - Num(H,i)] \tag{5.32}$$

We denote expressions like Eq. 5.31 as ModPadé(H,i,j;m,k).

In the figure below we plotted two ModPadé functions together with a numerical evaluation of the Glatting result (Eq. 5.25). We see that the higher order ModPadé approximants can replace the original function with a very good accuracy over the entire range of

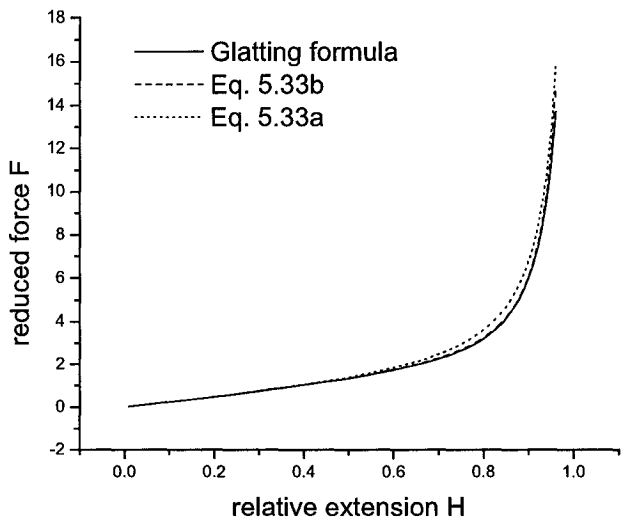


Fig. 5.3. The force-extension relations ModPadé(H,2,1;3,2) and ModPadé(H,7,2;8,6) are compared with the original result (Eq. 5.25) , for N=5.

extensions H, while the small order ones show some discernible errors for the intermediate stretching regime (see also Fig. 5.4). However, at the cost of slightly larger

errors, the latter ones would be preferable because of the much simpler analytical form. Indeed the two examples shown in Fig. 5.3 are given by

$$\langle F\rangle_{H(ModPade(H,2,1;3,2))} = \frac{3H}{1-H^2}\left[(1-1/N)-\frac{1}{3}H^2(1+1/N)\right] \tag{5.33a}$$

and

$$\begin{aligned}\langle F\rangle_{H(ModPade(H,7,2;8,6))} = \frac{3}{30625}H(&224021875N^2-904171500N+\\ &68015625-104002500H^2N^2+235347000H^2N+\\ &197068200H^2-16317000H^4N^2-6778800H^4N+\\ &159390000H^4-3534300H^6N^2-21009240H^6N+.\\ &93514392H^6-278135717H^7+29988175H^7N^2+\\ &1307290H^7N)/(N(7315N-22209-7785H^2N+\\ &22881H^2+470H^6N-672H^6))\end{aligned} \tag{5.33b}$$

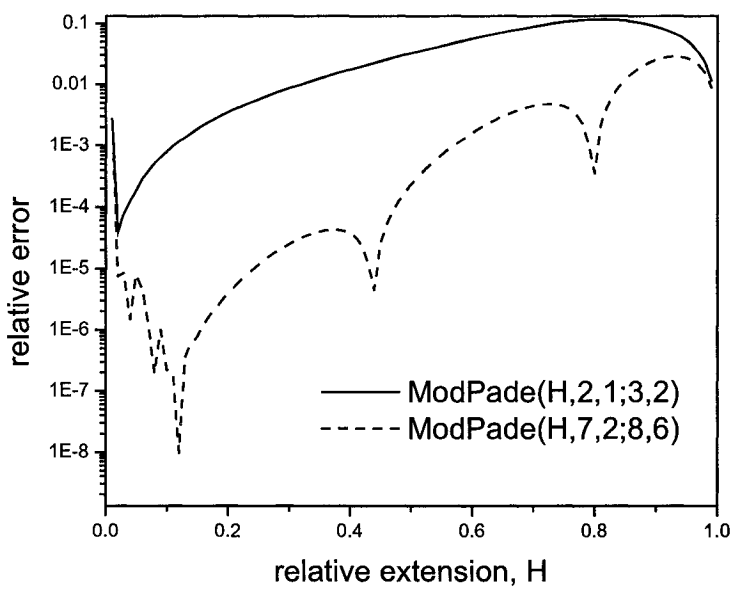


Fig.5.4 Semilogarithmic plot of the relative error for Eq. 5.33a (upper line) and Eq. 5.33b (lower line).

We note that the factor in front of the parenthesis in the Eq. 5.33a is the empirical Warner approximation (Eq. 5.22). In the small extension limit (H→0), we see that a correction term ∝1/N appears relative to the harmonic result, while the ModPadé approximant of the same precision, in the f-ensemble (Ref. 23)

$$F = \langle H \rangle_f \frac{3 - \langle H \rangle_f^2}{1 - \langle H \rangle_f^2} \tag{5.34}$$

recovers the harmonic limit for any value of N. The 1/N factor is thus what distinguises the two ensembles for finite-sized chains.

## *The distribution function and the mean equilibrium end-to-end distance*

We have shown in the first chapter that one of the most important results of the FJC model is that concerning the mean square end-to-end distance, i.e.

$$\langle h^2 \rangle = Nb^2 . \tag{5.35}$$

This is a general and exact result, obtained from geometrical considerations, namely the hypothesis regarding the independence of the segments in the chain. It holds for any N and for any particular potential energy between the sub-segments of each FJC segment. But only the harmonic limit (Gaussian chain or FJC with N large), through the Gaussian probability distribution of h, is strictly compatible with the above result when using the usual definition of the statistical mean of a random variable, i.e.

$$\langle h^2 \rangle = \int h^2 W(h) dh . \tag{5.36}$$

When the contractile force is anharmonic, the two approaches, geometric and statistical, lead to a different result for $\langle h^2 \rangle$. Certainly, they converge at large N, when the FJC probability distribution function for h can be well approximated by the Gaussian one.

In the light of the above statements, we now derive the probability distribution for the force-extension relation that we found in the previous section (Eqs. 5.33). With the reduced variables this can be written as a Boltzmann distribution

$$W(H) = \frac{H^2 e^{-U(H)}}{\int_0^1 H^2 e^{-U(H)} dH} \tag{5.37}$$

The scaled potential U is related to the reduced force by integration

$$U(H) = N \int_0^H \langle F \rangle_{H'} \, dH' \tag{5.38}$$

Finally the mean square end-to-end distance of the chain can be calculated with

$$\langle H^2 \rangle = \int_0^1 H^2 W(H) dH \tag{5.39}$$

For example, if N=10 we obtain $\langle H^2 \rangle_{(\text{Eq. 5.33a})}$=0.099, while $\langle H^2 \rangle_{(\text{harmonic})}$=0.1. As expected, the anharmonic springs are slightly stiffer than the harmonic springs. At the same level of approximation, the f-ensemble gives $\langle H^2 \rangle_{(\text{Eq. 5.34})}$=0.089 (Ref. 23), which is clearly a much poorer approximation. It appears that a simple approximation on the type of Eq. 5.33a provides a very convenient analytical formula for the force-extension relation to be used in the h-ensemble. In particular, the exact FJC result $\langle h^2 \rangle = Nb^2$ is then well preserved.

Finally we emphasise the fact that the h-ensemble is the correct one that should be used for the Rouse chains. In the Rouse model is the spring extensions that are fixed followed then by the estimation of the forces on them. Conceptually this is the h-ensemble.

# Conclusions

The relaxation of complex systems is a field that is still opened to fundamental questions. One of the well-known facts is that the relaxational processes in an overwhelming number of macroscopic systems follow a stretched exponential function (or KWW relaxation). The common feature of these systems that is believed to be responsible for this relaxation behaviour is the disorder.

The subject of this thesis is the relaxation of linear disordered polymers. We studied the influence of a structural type of randomness on the relaxation dynamics of the polymers. Our results were interpreted using some of the theories that are relevant for the relaxation of disordered systems (the heterogeneous scenario and the competing exponential processes). A detailed presentation of these models was presented in the first part of the thesis.

We modified one of the most popular models for polymer solutions, the Rouse model (or spring-bead model), to introduce structural disorder. We randomized the spring constants along the polymer chain according to some specific probability distributions. The introduction of the spring randomness is legitimate in itself because of one the shortcomings of the Rouse model - the compositional polydispersity of many real polymers. For instance, the model could be appropriate for the study of random copolymers. Although some work has been done on the variation of the friction coefficient of the beads, there is no specific model, to our knowledge, that takes into consideration an elastic constant polydipersity. Our model considers four different types of distributions for the elastic spring constants. They are meant to represent various structural situations, some being closer to practical cases than others which are just of theoretical interest. For example, the uniform probability distribution is a convenient alternative to the popular Gaussian function, but the exponential one is merely chosen for the large probability of very small spring constant values (the anomalous distribution is essentially the opposite limit).

We studied the conformational relaxation dynamics of such random Rouse chains via the autocorrelation function of the end-to-end distance. From the mathematical point of view this is an random matrix eigenvalue problem. There is no exact analytical solution for this problem; therefore, a numerical study was required. For each random structure a symmetric matrix (the connectivity matrix) was obtained and the eigenvalues were binned to create a histogram representation of the relaxation spectrum. Our numerical study was performed with Matlab routines.

The characteristics of the spectra were analyzed for both one random realization (relaxation of a single disordered chain) and many realizations (relaxation of ensembles of random chains). At the single random chain level, the spectrum shows no significant differences from the standard Rouse chain, a fact that was clearly shown later when we looked at the correlation function itself. From the point of view of an ensemble, we found that the spectra display clear characteristics of non-exponential relaxation. These characteristics appear to different extend for the various ensembles we created. Indeed, our results for the corresponding correlation functions show KWW regimes for many of the cases. It is important to note that from an experimental point of view, these KWW time intervals would indeed be measurable. The characteristics of the KWW decay functions were analyzed further. The fact that the stretched exponent $\beta$ was molecular-size independent supported some experimental results (made on different systems) that revealed the stretched exponential universal character. Chains with different sizes relax in a similar way, although over different time intervals. It is only the type of randomness and its amplitude that affects the form of the relaxation. Therefore, the KWW parameter $\beta$ can be used as a test for the sample heterogeneity.

Finally, the finite size of the ensembles was studied. Our results indicate that the characteristics of the KWW regime depend on the size of the ensemble. Again, the system response varies from one type of disorder to the other: the KWW main parameter, the stretched exponential coefficient, undergoes important variations. Its decrease with the ensemble size could be interpreted as an extrinsic characteristic. Instead, we believe that it should be interpreted as a convergence towards a saturation value, which stands for infinitely large systems. On the other hand, this ensemble size dependence is a very relevant test for one of the actual microscopic theories that explain the emergence of the

stretched exponential relaxation, that is the theory of the competition between two exponential processes. According to this model, the differences between the KWW regimes observed for the various distribution functions are due to the shape of the low-end of the eigevalue spectrum. Our results clearly show that the four cases produced rather different spectra indeed.

The subject of the last part of the thesis is related to the elasticity of single polymeric chains. Recent experimental breakthroughs that make possible single DNA molecule manipulations, for example, ask for equivalent progress on the theoretical side. Here we made a detailed presentation of the two different statistical ensembles used to describe the force-extension relation. The strain ensemble poses important mathematical challenges. We proposed a method that simplifies in a large measure one of the recently proposed approximations. This method, which uses a polynomial ratio approximation, offers a good alternative to the original result because it greatly reduces the computation times. The algorithm offers a controllable precision and preserves quite well the original scaling properties.

# Appendix:
# The partition function for the generalized FJC (Ref. 24)

For a chain of M+1 mass points with positions $\vec{R}_i$ (i=0,1,..., M), the general partition function $Z_h$ in the h-ensemble is given by

$$Z_h = \int d\{\vec{R}\} \exp[-U(\{\vec{R}_i\})/k_B T]\,\delta(\vec{R}_0)\,\delta(\vec{h} - (\vec{R}_M - \vec{R}_0)) \,. \qquad \text{(A2.1)}$$

Although the complete partition function includes the kinetic energy of the chain, in fact this contributes only with a constant to $Z_h$ and consequently does not influence the average force. All interactions are included in the potential energy U. This may include: the covalent bonds, the angle restrictions, the excluded volume interactions and various external fields. The first $\delta$ function fixes the first mass point at the origin of the coordinate system and the second one determines the end-to-end distance of the chain. Introducing the single bond vectors

$$\vec{b}_i = \vec{R}_i - \vec{R}_{i-1}, \quad i = 1,2,3,...M, \quad \vec{b}_0 = \vec{R}_0 \qquad \text{(A2.2)}$$

and integrating over $\vec{R}_0$, we get

$$Z_h(\vec{h}) = \int d\{\vec{b}_i\} \exp[-U(\{\vec{b}_i\})/k_B T]\,\delta(\vec{h} - \sum_{i=1}^{M} \vec{b}_i) \qquad \text{(A2.3)}$$

The freely jointed chain is introduced by dividing the chain into N independent and identical segments, each of them containing M/N single bonds. The length of the segments can vary, depending on the type of interaction between the bonds. Because there is no interaction potential between the segments, the expression in the integral above can be rewritten as a function of the new segments,

$$Z_h(\vec{h}) = \int d\{\vec{b}_j\} \exp[-\sum_{j=1}^{N} U_j(\{\vec{b}_i\})/k_B T]\,\delta(\vec{h} - \sum_{j=1}^{N} \vec{b}_j) \qquad \text{(A2.4)}$$

The index j identifies a specific freely-jointed segment $\vec{b}_j$, and in the summation above only the single bonds $\vec{b}_i$ of the j-th segment are included. The expression can be developed further and the index j in the segment potential U can be dropped because all the segments are identical

$$Z_h = \int\prod_{j=1}^{N} d\vec{b}_j [\int\prod_{i=1}^{M/N} d\vec{b}_i \exp(-U^1(\{\vec{b}_i\})/k_B T)\delta(\vec{b} - \sum_{i=1}^{M/N}\vec{b}_i)]\delta(\vec{h} - \sum_{j=1}^{N}\vec{b}_j) \qquad \text{(A2.5)}$$

where we can identify the quantity in square brackets with the segment partition function $s(\vec{b})$

$$s(\vec{b}_j) = \int\prod_{i=1}^{M/N} d\vec{b}_i \exp(-U^1(\{\vec{b}_i\})/k_B T)\delta(\vec{b}_j - \sum_{i=1}^{M/N}\vec{b}_i). \qquad \text{(A2.6)}$$

A further evaluation (Ref. 24) of this expression leads to the following form for the general partition function

$$Z_h \approx \left(\frac{(2\pi m k_B T)^{3(M-1)}}{(2\pi N)^3 \det(A)}\right)^{1/2} \exp\{-\frac{\beta h}{b} + N\ln[\int dbs(\vec{b})e^{\beta\vec{b}\cdot\vec{e}_h}]\} \qquad \text{(A2.7)}$$

where m is the mass of the segments and β is the solution of the following equation:

$$\bar{L}(\beta) \equiv \frac{\partial}{\partial\beta}\ln[\int d^3 bs(b)\exp(\beta\vec{b}\cdot\vec{e}_h)] = \frac{h}{N}. \qquad \text{(A2.8)}$$

A is a matrix whose entries are function of β.

The expression for the force can be now written using the derivative of the free energy:

$$\langle f\rangle_h = k_B T\left(\beta + \frac{1}{2}\frac{d}{dh}\ln[\det(A)]\right) \qquad \text{(A2.9)}$$

This is the partition function for the generalised freely-jointed chain with flexible bonds. It allows, at least in principle, the evaluation of the $Z_h$ function for different geometrical constrains. The lowest order approximation, when all the bonds are freely jointed, is considered here. In this case, the potential energy of a single segment is harmonic

$$u_1(\vec{b}) = \frac{k}{2}(b - b_0)^2 \qquad \text{(A2.10)}$$

where $b_0$ is the equilibrium length of a single bond. If the bonds are covalent, the elastic constant k is very large compared with $k_B T$ which makes possible the use the following approximation in the partition function $s(\vec{b})$:

$$s(\vec{b}) = \exp(-\frac{k}{2}(b - b_0)^2) \approx (\frac{2\pi k_B T}{k})^{1/2}\delta(b - b_0) \qquad \text{(A2.11)}$$

$$Z_h = (\frac{c}{A_{xx}A_{yy}A_{zz}})^{1/2}\exp\left\{-\frac{\beta h}{b} + N\ln[\frac{\sinh(\beta)}{\beta}]\right\} \qquad \text{(A2.12)}$$

where

$$A_{xx} = A_{yy} = b^2[\coth(\beta) - \frac{1}{\beta}]\frac{1}{\beta} \qquad A_{zz} = b^2\left[\frac{1}{(\beta)^2} - \frac{1}{\sinh^2(\beta)}\right] \quad \text{(A2.13)}$$

# Bibliography


1. Volkenstein, M.V. *Configurational statistic of polymeric chains*, Interscience Publishers, 1962

2. Doi, M. and Eduards, S.F. *The theory of polymer dynamics*, Clarendon Press, 1988

3. Doi, M. *Introduction to polymer physics*, Clarendon Press-Oxford, 1997

4. Flory, J.P. *Statistical mechanics of chain molecules*, Hanser Publishers, 1989

5. Ngay, K.L. in :Richert, R. and Blumen, A. (Eds) *Disorder effects on relaxational processes, glasses, polymers, proteins*, Springer-Verlag, 1994, pp. 89-150

6. Donth, E.J. *Relaxation and thermodynamics in polymers, glass transitions*, Akademie Verlag, 1992

7. Cai. C. and Chen, Z.Y. "Rouse dynamics of a dendrimer model in the θ condition, Macromolecules 30, 5104-5117 (1997)

8. Kemp, J. and Chen, Z.Y. "Nonexponential dynamic relaxation of randomly branched polymers in good solvents", Physical Review E, 56, 7017-7022 (1997)

9. Kemp, J. and Chen, Z.Y. "Semianalytical calculations of the rouse dynamics of randomly branched polymers", Physical Review E, 60, 2994-2998 (1999)

10. Palmer, R.G., Stein, D.L. and Anderson, P.W. "Models of hierarchically constrained dynamics for glassy relaxation", Physical Review Letters, 53, No.10 (1984)

11. Shlesinger, M. and Klafter, J. "The nature of temporal hierarchies underlying relaxation in disordered media", *Fractal in physics*, Pietronero, L. and Tossati, E. (editors), Elsevier Science Publishers B. V. (1986)

12. Klafter, J. and Shlesinger, M. "On the relationship among three theories of relaxation in disordered systems", Proc. Nat. Acad. Sci. USA, 83, 848-851 (1986)

13. Iori, G., Marinari, E. and Parisi, G. "Non-exponential relaxation time scales in disordered systems: An application to protein dynamics", Europhysics Letters, 25, 491-496 (1994)

14. Arbe, A., Colmenero, J., Monkenbusch, M. and Richter, D. "Dynamics of glass-forming polymers: "homogeneous" versus "heterogeneous" scenario", Physical Review Letters, 81, No.3 (1998)

15. Phillips, J.C. "Stretched exponential relaxation in molecular and electronic glasses", Rep. Prog. Phys. 59, 1133-1207 (1996)

16. Fukui, K. et al. "Analysis of eigenvalues and eigenvectors of polymer particles: random normal modes", Computational and theoretical Polymer Science, 11, 191-196 (2001)

17. Teraoka, I. *Polymer solutions An introduction to physical properties*, Wiley-Interscience, 2002

18. Tsang, K.Y. and Ngai K.L. "Relaxation in interacting arrays of oscillators", Physical review E, 54, R3067-R3070 (1996)

19. Rouse, P.E. "A theory of the linear viscoelastic proprieties of dilute solutions of coiling polymers", The Journal of Chemical Physics, 21, No.7, 1272-1280 (1953)

20. de Gennes, P.-G. "Relaxation anomalies in linear polymers", Macromolecules, 35, 3785-3786 (2002)

21. Ganazzoli, F., Rafaini, G. and Arrighi, V. "The stretched-exponential approximation to the dynamic structure factor in non-entangled polymer melt", Phys. Chem. Chem. Phys., 4, 3734-3742 (2002)

22. Laherrere, J. and Sornette, D. "Stretched exponential distributions in nature and economy: "fat tails" with characteristic scales", European Physics Journal B, 2, 525-539 (1998)

23. Slater, G.W., Hubert, S.J. and Nixon, G.I. "Construction of approximate entropic forces for finitely extensible nonlinear elastic (FENE) polymers", Macromol. Theory Simul., 3, 695-704 (1994)

24. Glatting, G., Winkler, R.G. and Reineker, P. "Partition function and force extension relation for a generalized freely jointed chain", 26, 6085-6092 (1993)

25. Titantah. J.T., Pierleoni, C. and Ryckaert, J.-P. "Different statistical mechanical ensembles for a stretched polymer", Physical Review E, 60, No.6, 7010-7021 (1999)

26. Lavery, R. et al. "Structure and mechanics of single biomolecules: experiment and simulation", Journal of Physics Condensed Matter, 14, R383-R414 (2002)

27. Flory, P. *Principles of Polymers Chemistry*, Cornell University Press, 1953

28. von Ferber, C. and Blumen, A. "Dynamics of dendrimers and of randomly bulit brabched polymers", Journal of Chemical Physics, 116, No.19 (2002)

29. Cowie, J.M. et.al. "Physical aging in poly(vinyl acetate).2. relative rates of volume and enthalpy relaxation", Macromolecules, 31, 2611 (1998)

30. Smith, S.B., Finzi, L. and Bustamante, C. Science 258, 1122-1126 (1992)

31. Keller.D, Swigon,D. and Bustamante, C. "Relating single-molecule measurements to thermodynamics", Biophysical Journal, 84, 733-738 (2003)

32. Makarov, D.E. and Wang, Z. "On the interpretation of force extension curves of single protein molecules", Journal of Chemical Physics, 116, No.17, 7760-7765 (2002)

33. Kreuzer, H.J. and Payne, S. H. "Stretching a macromolecule in an atomic force microscope: Statistical mechanical analysis", Physical Review E, 63, 021906 (2001)

34. Blunde, A et. All. "Anomalous size dependence of relaxational precesses", Physical Review Letters, 78, No.17 (1997)

35. Satmarel, C., Gurtovenko, A.A. and Blumen, A. "Viscoelastic relaxation of cross-linked, aleternating copolymers in the free-daining limit", Macromolecules, 36, 486-4944 (2003)

36. Meiss, JD and Ott E. Physics Review Letter 55, 2741 (1985)

37. Kohlrausch, R, Ann. Phys. (Leipzig) 12, 393 (1847)

38. Williams, G. and Watts, D.C., Trans. Faraday Soc. 66, 80 (1970)

39. Cowan, G. *Statistical data analysis: with applicationns from particle physics*, Oxford Science Publications, 1998